Article

Developmental Cell

S-acylation of the Wnt receptor Frizzled-5 by zDHHC5 controls its cellular localization and synaptogenic activity in the rodent hippocampus

Graphical abstract

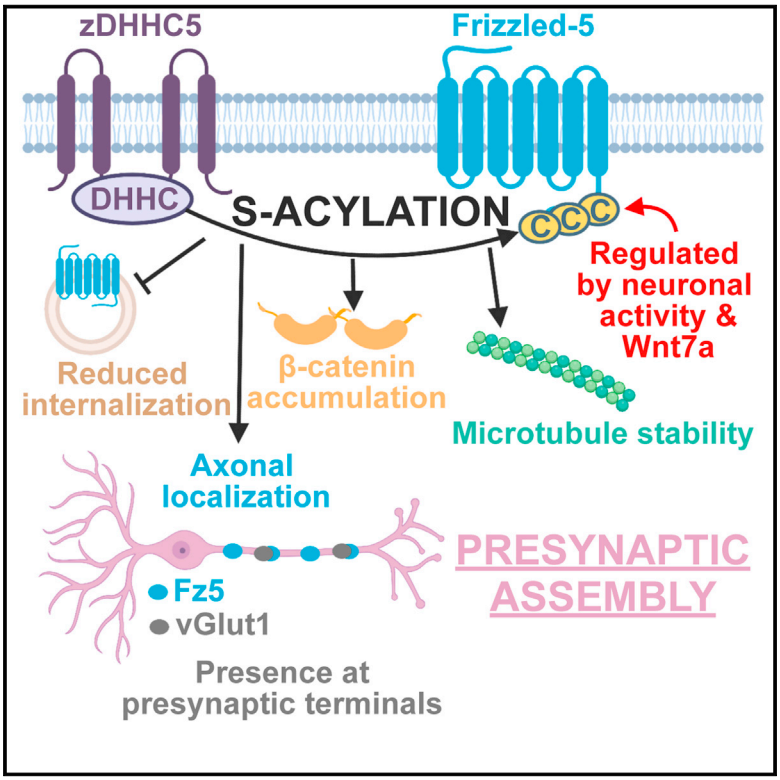

Authors

Samuel Teo, Alessandro Bossio, Eleanna Stamatakou, Patricia Pascual-Vargas, Megan E. Jones, Laura-Nadine Schuhmacher, Patricia C. Salinas

Correspondence

p.salinas@ucl.ac.uk

In brief

How receptors for synaptogenic factors are localized is not well understood. Teo, Bossio, Stamatakou et al. found that the key Wnt receptors Frizzled are post-translationally S-acylated, and this controls their localization to the cell surface, along axons, and to presynaptic sites, thus having an impact on Wnt signaling and presynaptic function.

Highlights

- Frizzled receptors are S-acylated, including Fz5 at its 3 C-terminal cysteines
- zDHHC5 S-acylates Fz5, a process mediated by neuronal activity and Wnt7a ligand
- Fz5 S-acylation controls its localization to the cell surface and along axons
- S-acylation-deficient Fz5 receptor fails to promote presynaptic assembly *in vivo*

Teo et al., 2023, Developmental Cell *58*, 1–17
October 23, 2023
https://doi.org/10.1016/j.devcel.2023.07.012

CellPress

Developmental Cell

CellPress
OPEN ACCESS

Article

S-acylation of the Wnt receptor Frizzled-5 by zDHHC5 controls its cellular localization and synaptogenic activity in the rodent hippocampus

Samuel Teo,[1,2] Alessandro Bossio,[1,2] Eleanna Stamatakou,[1,2] Patricia Pascual-Vargas,[1] Megan E. Jones,[1] Laura-Nadine Schuhmacher,[1] and Patricia C. Salinas[1,3,*]

[1]Department of Cell and Developmental Biology, Division of Biosciences, University College London, London WC1E 6BT, UK
[2]These authors contributed equally
[3]Lead contact
*Correspondence: p.salinas@ucl.ac.uk
https://doi.org/10.1016/j.devcel.2023.07.012

SUMMARY

Proper localization of receptors for synaptic organizing factors is crucial for synapse formation. Wnt proteins promote synapse assembly through Frizzled (Fz) receptors. In hippocampal neurons, the surface and synaptic localization of Fz5 is regulated by neuronal activity, but the mechanisms involved remain poorly understood. Here, we report that all Fz receptors can be post-translationally modified by S-acylation and that Fz5 is S-acylated on three C-terminal cysteines by zDHHC5. S-acylation is essential for Fz5 localization to the cell surface, axons, and presynaptic sites. Notably, S-acylation-deficient Fz5 is internalized faster, affecting its association with signalosome components at the cell surface. S-acylation-deficient Fz5 also fails to activate canonical and divergent canonical Wnt pathways. Fz5 S-acylation levels are regulated by the pattern of neuronal activity. *In vivo* studies demonstrate that S-acylation-deficient Fz5 expression fails to induce presynaptic assembly. Our studies show that S-acylation of Frizzled receptors is a mechanism controlling their localization and function.

INTRODUCTION

Synapse assembly is crucial for the formation of functional neuronal circuits. This process is modulated by signaling molecules and neuronal activity.[1–4] Receptors for synaptogenic organizers are distributed along neurites and then become localized to future synaptic sites. However, the molecular mechanisms that control the trafficking, localization, and function of these receptors remain poorly understood.

The Wnt family of secreted proteins are synaptogenic signals that modulate the formation of neuronal connections by binding to surface Wnt receptors, activating different downstream signaling cascades.[5–7] The most studied Wnt receptors are Frizzled (Fz), a family of seven-transmembrane receptors.[8,9] The binding of Wnts to Fz receptors triggers the activation of different Wnt signaling cascades that promote a variety of cellular functions.[10] These pathways include canonical Wnt signaling that inhibits glycogen synthase kinase-3 (GSK3) to stabilize β-catenin and activate T cell factor (TCF)-mediated transcription[11,12] and the Wnt/divergent canonical pathway that modulates the microtubule cytoskeleton through GSK3.[13] Non-canonical Wnt signaling pathways include the planar cell polarity pathway required for tissue and cell polarity[14,15] and the Wnt/Ca^{2+} pathway that plays an important role during embryogenesis and post-natal development.[5,7] In the mammalian nervous system, Fz receptors regulate many processes including axon guidance, dendritogenesis, synapse formation, synaptic transmission, and synaptic plasticity.[16–19] For example, Wnt7a promotes the assembly of pre- and post-synaptic sites through Fz5 and Fz7, respectively.[20,21] Importantly, Wnt7a-Fz5 signaling is essential for both basal and activity-induced presynaptic assembly in hippocampal neurons. Indeed, Fz5 surface localization is regulated by the pattern of neuronal activity, as high-frequency stimulation (HFS) increases whereas low-frequency stimulation (LFS) decreases surface Fz5.[20] HFS also promotes Fz5 localization to synapses, a process modulated by Wnts.[20] However, the molecular mechanisms underpinning Fz5 trafficking and localization remain to be elucidated.

The trafficking and localization of proteins are regulated by post-translational modifications (PTMs). A prominent modification present in synaptic proteins is S-acylation, the reversible covalent attachment of fatty acids to cysteine residues.[22,23] S-acylation renders proteins more hydrophobic, altering their localization and targeting them to specific membrane domains where they exert their functions.[24] S-acylation also controls protein turnover,[25,26] trafficking, and sorting to specific subcellular compartments.[27,28] Furthermore, S-acylation regulates protein-protein interactions such as ligand-receptor binding and interactions with scaffold proteins or signalosome components.[23,29] Thus, protein S-acylation affects diverse cellular functions. In the nervous

Please cite this article in press as: Teo et al., S-acylation of the Wnt receptor Frizzled-5 by zDHHC5 controls its cellular localization and synaptogenic activity in the rodent hippocampus, Developmental Cell (2023), https://doi.org/10.1016/j.devcel.2023.07.012

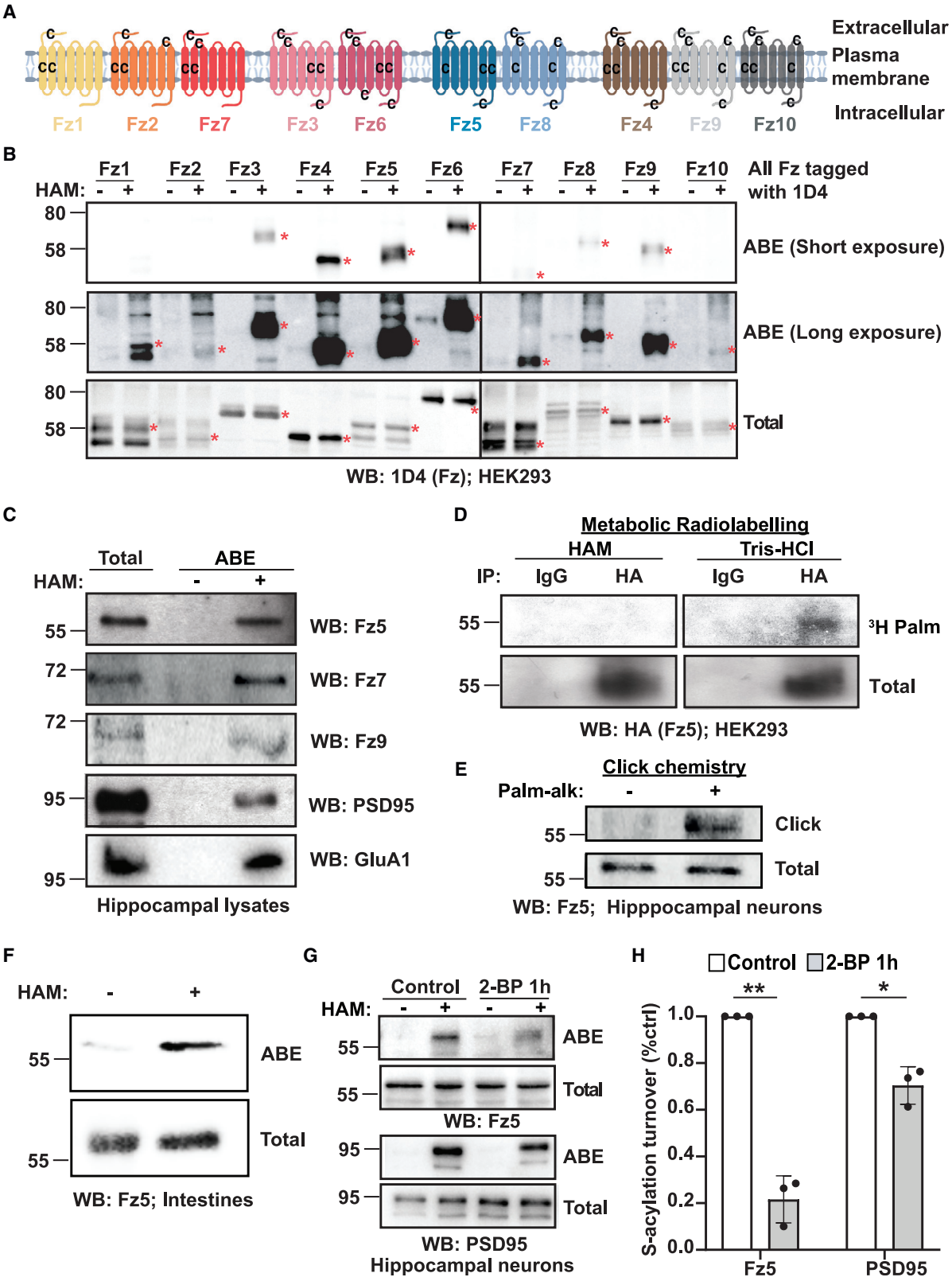

(legend on next page)

Please cite this article in press as: Teo et al., S-acylation of the Wnt receptor Frizzled-5 by zDHHC5 controls its cellular localization and synaptogenic activity in the rodent hippocampus, Developmental Cell (2023), https://doi.org/10.1016/j.devcel.2023.07.012

system, aberrant protein S-acylation has been linked to neurological diseases such as Alzheimer's disease, schizophrenia, intellectual disability, and major depressive disorder.[30,31]

Here, we investigated whether Fz receptors are S-acylated, focusing on Fz5 given its role at the synapse[20] and analyzed the impact of Fz5 S-acylation on its function. Our bioinformatics and biochemical analyses revealed that all Fz receptors can be S-acylated. We demonstrated that Fz5 is S-acylated on its C terminus by the acyltransferase zAsp-His-His-Cys(DHHC)5. Fz5 S-acylation is dependent on the pattern of neuronal activity and is necessary for its retention at the plasma membrane and its localization along the axon and to presynaptic sites. Fz5 S-acylation also regulates signaling through the canonical and divergent canonical Wnt pathways. *In vivo* expression of an S-acylation-deficient Fz5 receptor demonstrated that this PTM is required for Fz5 synaptogenic function in the hippocampus. Our studies uncover the presence of a lipid modification on Fz receptors and define a molecular mechanism that regulates the localization and function of these important Wnt receptors. Our findings open more avenues to modulate Wnt signaling through Fz receptors in health and disease.

RESULTS

Frizzled receptors are S-acylated

S-acylation is a PTM present in many synaptic proteins and regulates their synaptic localization.[30,32] Given that Fz receptors are present at synapses, we examined whether these receptors are S-acylated. We used the GPS Palm 2021 software,[33] a deep-learning-based graphic presentation system, and found that all human Fz receptors were predicted to be S-acylated on multiple cysteines (Table S1). Fz receptors across different subfamilies[9] exhibited a similar distribution of putative S-acylation sites that spread across various protein domains including the N-terminal, transmembrane, juxtamembrane, and C-terminal domains (Figure 1A). Next, we tested whether Fz receptors are S-acylated by performing acyl-biotin exchange (ABE) analyses (Figure S1A). We expressed Fz receptors tagged with 1D4 in HEK293 and clearly detected Fz3-6 and Fz9 S-acylation (Figure 1B). In contrast, Fz1, Fz7, and Fz8 exhibited lower S-acylation levels, and weak signals were observed for Fz2 and Fz10 (Figure 1B). Taken together, these bioinformatic and biochemical analyses suggest that all Fz receptors can be S-acylated.

We next investigated if Fz receptors that play a role in synapse assembly are S-acylated endogenously in the hippocampus. These receptors include Fz5 and Fz7 that are required for Wnt7a-mediated synaptogenic activity on the pre-[20] and post-synaptic[21] sides respectively and Fz9, which is required for Wnt5a-mediated synaptogenesis.[34] Indeed, ABE analyses on mouse hippocampal lysates revealed that all three Fz receptors (Fz5, Fz7, and Fz9) were endogenously S-acylated (Figure 1C). Consistent with previous reports,[35,36] we also confirmed that PSD95 and the GluA1 subunit of α-amino-3-hydroxy-5-methyl-4-isoxazolepropionic acid receptors (AMPARs) were S-acylated (Figure 1C). Together, our studies show that endogenous Fz receptors are S-acylated in the brain.

Different approaches demonstrate Fz5 S-acylation

Our subsequent studies focused on Fz5 as this receptor is required for Wnt7a-mediated synaptogenic activity and its surface and synaptic levels are modulated by neuronal activity.[20] We hypothesized that S-acylation might have a role in these processes as this PTM regulates the localization of a large number of synaptic proteins.[30,32] To further confirm that Fz5 is S-acylated, we used two additional methods. First, we detected the metabolic incorporation of radioactive palmitate (Figure S1B) into *Fz5*-hemagglutinin (*HA*)-expressing HEK293 (Figure 1D). In contrast, hydroxylamine (HAM) treatment removed the palmitate groups and the radioactivity signal (Figure 1D). Second, we performed click chemistry (Figure S1C) in hippocampal neurons and showed that the alkynyl analog of palmitic acid was incorporated into endogenous Fz5 receptors (Figure 1E). These results demonstrate that palmitic acid can be incorporated into Fz5, suggesting that Fz5 is S-palmitoylated, a subtype of S-acylation that specifically attaches palmitate (C16) to cysteines.[24] Thus, we demonstrate that Fz5 is S-acylated using three different methods.

We also investigated whether Fz5 S-acylation occurs in non-neuronal tissues. In mouse intestines, a tissue with high Fz5 expression,[37] we detected endogenous Fz5 S-acylation (Figure 1F), suggesting that Fz5 S-acylation is not specific to neuronal tissues and could play important functions in other tissues.

Subsequently, we examined endogenous Fz5 S-acylation turnover in neurons. As this PTM is reversible, the length of time a protein is S-acylated could affect its localization

Figure 1. Frizzled receptors including Fz5 are S-acylated

(A) Schematic diagram of Frizzled receptor subfamilies and their putative S-acylation sites ("C") using the GPS Palm 2021 software. 'C' represents one or more cysteines.

(B) ABE assays from *Frizzled-1D4*-expressing HEK293. Samples were run on two membranes shown side by side with different exposures. Red asterisks indicate the bands corresponding to Fz receptors (n = 3 cultures).

(C) ABE assays from mouse hippocampal lysates showed endogenous Fz5, Fz7, and Fz9 S-acylation. PSD95 and GluA1 were positive controls (n = 3 animals).

(D) Metabolic incorporation of radioactive palmitate (^{3}H-Palm) into *Fz5-HA*-expressing HEK293 followed by immunoprecipitation (IP) with anti-HA antibody. IgG was an IP negative control. Hydroxylamine (HAM) treatment released radioactive palmitate and was a negative control (n = 3 cultures).

(E) Click chemistry assays in hippocampal neurons detected the incorporation of palmitic acid-alkyne at endogenous Fz5 receptors (n = 3 cultures).

(F) ABE assays from mouse intestinal lysates showed endogenous Fz5 S-acylation (n = 3 animals).

(G) ABE assays from hippocampal neurons for S-acylated Fz5 and PSD95 after 1-h exposure to vehicle control or 2-BP.

(H) Quantification of (G) for Fz5 and PSD95 S-acylation turnover (n = 3 cultures, separate one-sample t tests).

For (B), (C), (F), and (G), samples were treated with hydroxylamine (+HAM) or vehicle control (negative controls, −HAM) for ABE assays.

For (E), samples were treated with palmitic acid-alkyne (+palm-alk) or vehicle (negative controls, −palm-alk) for click chemistry assays.

Molecular weights (kDa) are indicated on the left of membranes.

Data expressed as mean ± SD. Statistics: *$p < 0.05$, **$p < 0.01$.

See also Figures S1A–S1E and Table S1.

Please cite this article in press as: Teo et al., S-acylation of the Wnt receptor Frizzled-5 by zDHHC5 controls its cellular localization and synaptogenic activity in the rodent hippocampus, Developmental Cell (2023), https://doi.org/10.1016/j.devcel.2023.07.012

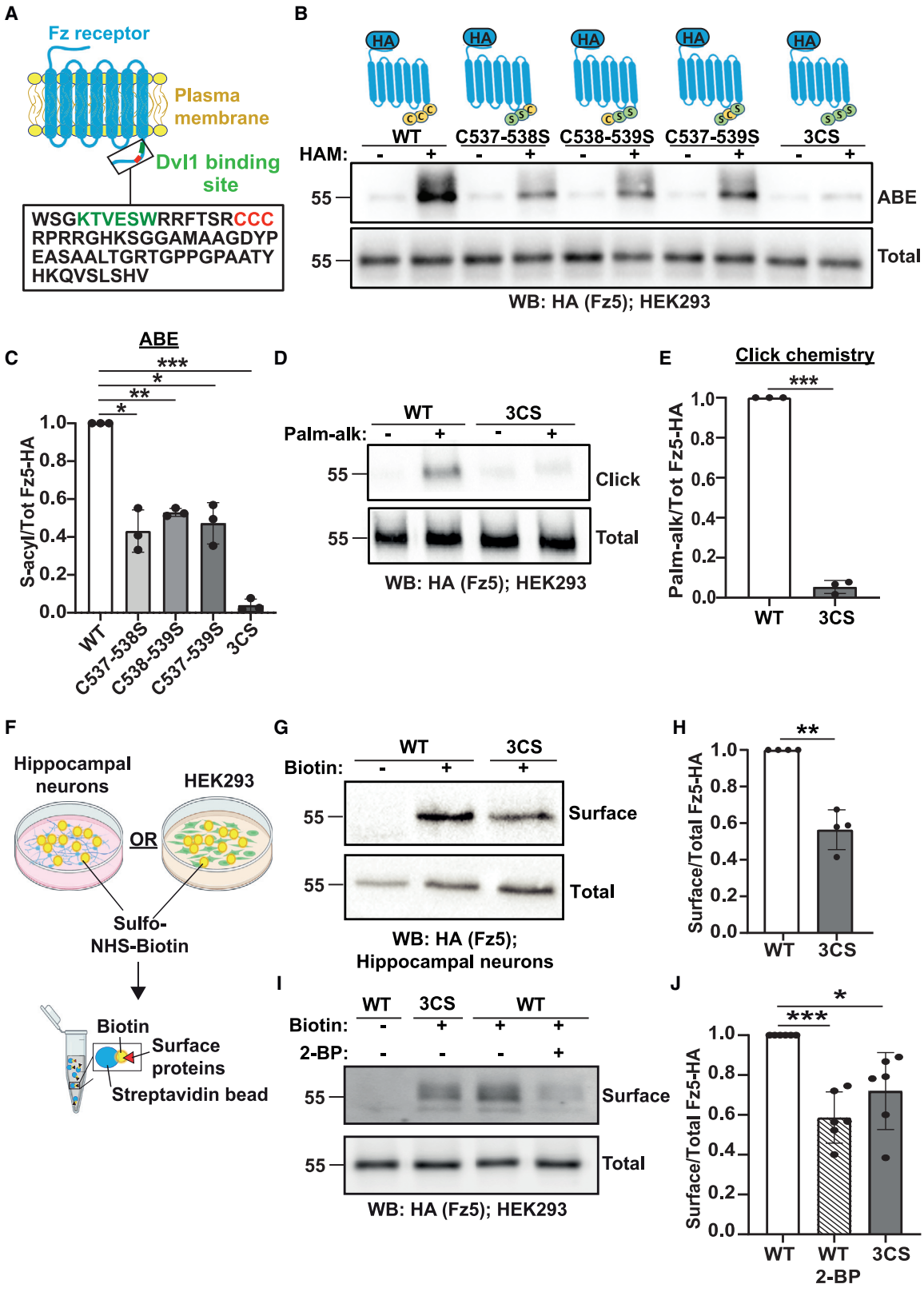

Figure 2. Fz5 is S-acylated on three cysteine sites of its C terminus, and this modification regulates Fz5 levels at the cell surface

(A) Schematic diagram depicting the human Fz5 C terminus containing the Dvl1 binding domain (green) and three S-acylated cysteines (red).

(B) Schematic diagram of Fz5-HA double and triple (3CS) mutants, and ABE assays of their Fz5-HA S-acylation levels.

(legend continued on next page)

Please cite this article in press as: Teo et al., S-acylation of the Wnt receptor Frizzled-5 by zDHHC5 controls its cellular localization and synaptogenic activity in the rodent hippocampus, Developmental Cell (2023), https://doi.org/10.1016/j.devcel.2023.07.012

and/or function.[38] We exposed hippocampal neurons to 2-bromopalmitate (2-BP), a non-metabolizing analog of palmitic acid that is widely used to block S-acylation.[39] 2-BP significantly reduced Fz5 S-acylation (80% decrease) after 1 h (Figures 1G and 1H). In contrast, 2-BP decreased PSD95 S-acylation levels by 30%, suggesting that PSD95 exhibits longer-lasting S-acylation than Fz5 (Figures 1G and 1H). We also used a newly developed S-acylation inhibitor, cyano-myracrylamide (CMA), which is thought to have fewer off-targets than 2-BP.[40] Exposure of neurons to CMA for 6 h led to a 60% decrease in S-acylated Fz5 and a 20% decrease in S-acylated PSD95 (Figures S1D and S1E). Together, these findings demonstrate that endogenous Fz5 is S-acylated in neurons and that its S-acylation is relatively less stable than in PSD95.

Fz5 is S-acylated on its C-terminal domain

Next, we asked which cysteine sites on Fz5 are S-acylated. We focused on the putative S-acylation sites predicted by the GPS Palm 2021 software.[33] Specifically, we examined the three Fz5 cysteine sites (C537, C538, and C539) on its C terminus with high S-acylation prediction scores (Table S1). This domain is important for signaling by binding to Dishevelled1 (Dvl1), a scaffold protein and key component of the Wnt signalosome.[41] Of note, these three cysteine residues are near (6 amino acids away) to one of the Dvl1-binding motifs[42] (Figure 2A). We generated several Fz5-HA mutants (C537S, C538S, and C539S) where two of the three cysteines were mutated to serine, leaving one C-terminal cysteine available for S-acylation (Figure 2B). We also replaced all three cysteines with serine, resulting in a mutant (three cysteine residues replaced by serines [3CS]) with no C-terminal cysteines available for S-acylation (Figure 2B). By using the ABE assay, we found that mutation of any two of the three cysteines on the Fz5 C terminus significantly decreased S-acylation levels of this receptor (Figure 2C). Importantly, mutation of all three cysteines almost completely abolished Fz5 S-acylation (Figure 2C). To validate our finding that the 3CS mutant is S-acylation deficient, we performed click chemistry in HEK293 expressing wild type (*WT*)-*Fz5-HA* or *3CS-Fz5-HA* (Figure 2D). WT-Fz5 S-acylation was detected using this method, whereas 3CS-Fz5 exhibited almost no S-acylation (Figure 2E). Together, our results demonstrate that the C terminus of Fz5 could be S-acylated on each of the three adjacent cysteine residues.

S-acylation regulates Fz5 localization at the plasma membrane

What is the role of Fz5 S-acylation? As this PTM controls protein localization to the cell surface,[22,24] we evaluated whether S-acylation regulates Fz5 levels at the plasma membrane. Surface biotinylation experiments (Figure 2F) revealed a significant reduction in the level of 3CS-Fz5 at the cell surface when compared with WT-Fz5 in both hippocampal neurons (Figures 2G and 2H) and HEK293 (Figures 2I and 2J), without affecting total Fz5 levels. Consistently, inhibition of S-acylation with 2-BP decreased Fz5 surface levels in HEK293 expressing *WT-Fz5-HA* receptor (Figures 2I and 2J). We also performed live staining in hippocampal neurons expressing *WT-Fz5-HA* or *3CS-Fz5-HA* to evaluate surface Fz5-HA (sFz5-HA) levels (Figures S1F and S1H). Confirming our surface biotinylation results, we observed a significant decrease in 3CS-sFz5 compared with WT-sFz5 at axons (Figure S1G) and dendrites (Figure S1I). These results demonstrate that deficiency in Fz5 S-acylation reduces its surface levels.

The finding that S-acylation regulates Fz5 surface levels suggests that this PTM is important for the activation of the Wnt cascade initiated at the plasma membrane. We first investigated whether S-acylation affects the interaction between Fz5 receptors as these receptors form dimers and oligomerize at the plasma membrane.[43,44] We performed co-immunoprecipitation (coIP) experiments in HEK293 to evaluate WT-Fz5;WT-Fz5 or 3CS-Fz5;3CS-Fz5 interaction (Figure S2A). Receptors were super-ecliptic pHluorin (SEP) or HA tagged. However, no significant differences were detected between the interaction of WT-Fz5 or 3CS-Fz5 with Fz5 receptors of the same type (Figure S2B). Thus, despite reduced 3CS-Fz5 surface levels, Fz5;Fz5 dimerization is unaffected.

Next, we asked whether Fz5 S-acylation affects its interaction with the Wnt co-receptor low-density lipoprotein (LDL)-receptor-related protein 6 (LRP6), a step required for canonical Wnt signaling.[45] Cells were exposed to BSA vehicle control or recombinant Wnt7a, as the interaction of Fz5 with LRP6 is increased by Wnts.[46,47] Lysates from HEK293 expressing *WT-Fz5-HA* plus *LRP6* or *3CS-Fz5-HA* plus *LRP6* treated with Wnt7a or BSA vehicle control (Figure S2C) were used to perform coIP experiments (Figure S2D). The interaction between 3CS-Fz5 and LRP6 was significantly lower when compared with WT-Fz5 and LRP6 under basal conditions (Figures S2E and S2F). Importantly,

(C) Quantification of (B) for Fz5-HA S-acylation of each mutant normalized to WT levels (n = 3 cultures, Kruskal-Wallis with Games-Howell post hoc).
(D) Click chemistry assays from HEK293 expressing *WT-Fz5-HA* or *3CS-Fz5-HA* to detect palmitic acid-alkyne incorporation.
(E) Quantification of (D) for incorporated palmitic acid-alkyne levels at WT-Fz5-HA or 3CS-Fz5-HA (n = 3 cultures, one-sample t test).
(F) Diagram showing surface biotinylation with membrane impermeable sulfo-NHS-biotin in hippocampal neurons or HEK293. Biotinylated surface proteins were pulled down with streptavidin beads.
(G) Surface biotinylation analyses of WT-Fz5-HA or 3CS-Fz5-HA in hippocampal neurons.
(H) Quantification of (G) for 3CS-Fz5-HA surface levels normalized to WT-Fz5-HA (n = 4 cultures, one-sample t test).
(I) Surface biotinylation analyses of HEK293 expressing *WT-Fz5-HA* or *3CS-Fz5-HA*. *WT-Fz5-HA*-expressing cells were treated for 60 min with vehicle control or 2-BP.
(J) Quantification of (I) for Fz5-HA surface levels normalized to vehicle control-treated WT-Fz5-HA (n = 6 cultures, Kruskal-Wallis with Dunn's post hoc).
For (B), samples were treated with hydroxylamine (+HAM) or vehicle control (negative controls, −HAM) for ABE assays.
For (D), samples were treated with palmitic acid-alkyne (+palm-alk) or vehicle (negative controls, −palm-alk) for click chemistry assays.
For (G) and (I), samples were treated with (+biotin) or without (negative controls, −biotin) sulfo-NHS-biotin for surface biotinylation assays.
Molecular weights (kDa) are indicated on the left of membranes.
Data expressed as mean ± SD. Statistics: *p < 0.05, **p < 0.01, ***p < 0.001.
See also Figures S1F–S1I and S2. NHS, N-hydroxysuccinimide.

Please cite this article in press as: Teo et al., S-acylation of the Wnt receptor Frizzled-5 by zDHHC5 controls its cellular localization and synaptogenic activity in the rodent hippocampus, Developmental Cell (2023), https://doi.org/10.1016/j.devcel.2023.07.012

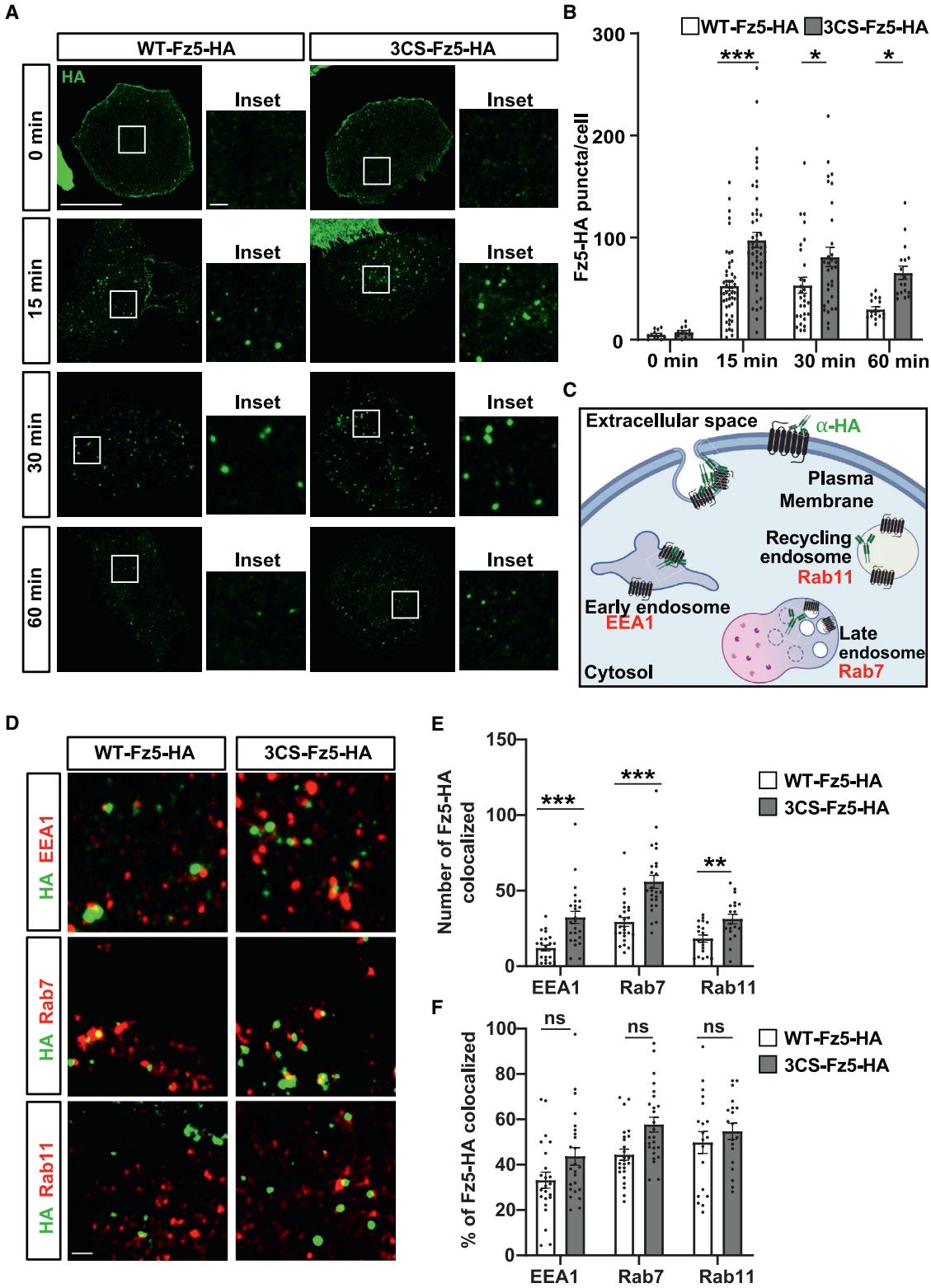

Figure 3. S-acylation reduces Fz5 endocytosis without affecting its transit through the endocytic pathway

(A) Confocal images of NRK cells expressing *WT-Fz5-HA* or *3CS-Fz5-HA* without anti-HA antibody internalization (0 min) and 15, 30, or 60 min after antibody internalization. Insets show digitally magnified images of white boxes. Fz5-HA (green). Scale bars: 25 μm (main) and 2 μm (insets).

(B) Quantification of (A) for the number of Fz5-HA endocytic puncta (n = 12–50 cells, two-way ANOVA with Bonferroni's post hoc).

(legend continued on next page)

Please cite this article in press as: Teo et al., S-acylation of the Wnt receptor Frizzled-5 by zDHHC5 controls its cellular localization and synaptogenic activity in the rodent hippocampus, Developmental Cell (2023), https://doi.org/10.1016/j.devcel.2023.07.012

Wnt7a significantly increased the interaction between WT-Fz5 and LRP6 (Figures S2E and S2F). In contrast, Wnt7a had no significant effect on the interaction between 3CS-Fz5 and LRP6 (Figures S2E and S2F). The decreased level of the receptor complex between 3CS-Fz5 and LRP6 is consistent with our finding that fewer Fz5 S-acylation-deficient receptors are present at the cell surface.

We also examined if S-acylation affects the interaction between Fz5 and Dvl1, the scaffold protein recruited to the plasma membrane as an early event in all Wnt signaling cascades.[42] We performed coIP experiments to determine the interaction between WT-Fz5-SEP or 3CS-Fz5-SEP and Dvl1-HA (Figure S2G). The interaction between 3CS-Fz5 and Dvl1 was approximately 35% lower when compared with WT-Fz5 and Dvl1 (Figure S2H), consistent with the decreased level of 3CS-Fz5 at the cell surface. Together, our results suggest that S-acylation regulates Fz5 surface levels, promoting Fz5 interaction with LRP6 and Dvl1 at the plasma membrane.

Fz5 S-acylation regulates receptor endocytosis

How does S-acylation affect Fz5 surface levels? S-acylation can positively or negatively regulate protein internalization.[48,49] We therefore asked whether reduced 3CS-Fz5 surface levels were due to increased receptor internalization by performing antibody feeding experiments. In normal rat kidney (NRK) cells expressing *WT-Fz5-HA* or *3CS-Fz5-HA*, we examined Fz5-HA endocytic cluster formation at 0 (no internalization), 15, 30, and 60 min after internalization (Figure 3A). At all time points, significantly more 3CS-Fz5 puncta were internalized compared with WT-Fz5 (Figure 3B). These findings demonstrate that Fz5 S-acylation regulates receptor endocytosis.

We next evaluated the transit of internalized Fz5 receptors through the endocytic pathway. The most pronounced difference in the number of 3CS-Fz5 endocytic clusters compared with WT-Fz5 was observed at 15 min post-internalization (Figure 3B). Therefore, we examined the presence of common markers of early, late, and recycling endosomes (EEA1, Rab7, and Rab11, respectively) at this time point (Figure 3C). Indeed, Fz5-HA clusters colocalized with each of these markers (Figure 3D). Consistent with increased 3CS-Fz5 endocytosis, significantly more 3CS-Fz5 puncta colocalized with all three endocytic markers compared with WT-Fz5 (Figure 3E). To account for the difference in the total number of endocytic Fz5-HA puncta, we assessed the percentage of receptor colocalizing with each endocytic marker to evaluate its transit through the endocytic pathway. We observed no significant differences between the percentage of WT-Fz5 or 3CS-Fz5 clusters that colocalized with all three endosomal markers (Figure 3F). Thus, S-acylation regulates Fz5 endocytosis without affecting its transit through the endocytic pathway.

The surface levels of receptors also depend on their lateral mobility at the plasma membrane, a process S-acylation can regulate.[50] We examined this process by fluorescence recovery after photobleaching (FRAP) in NRK cells expressing *WT-Fz5* or *3CS-Fz5* (Figure S3A). These receptors were tagged at the N terminus with SEP, a pH-sensitive GFP variant that is fluorescent only at neutral pH, which is normally found in the extracellular space, but not at the acidic pH of intracellular vesicles.[51] After photobleaching, recovery of fluorescence intensity is achieved by lateral diffusion of nearby receptors and/or by the insertion of receptors from intracellular stores.[52] As we only photobleached a small area (18 μm^2) and recorded for a short time (103.18 s), Fz5-SEP fluorescence recovery could be attributed to lateral diffusion as minimal exocytosis would have occurred under these conditions. FRAP and the percentage of mobile and immobile receptors were similar between WT-Fz5 and 3CS-Fz5 (Figures S3B and S3C), suggesting that Fz5 S-acylation does not affect its lateral mobility.

We next evaluated the protein stability of WT-Fz5 versus 3CS-Fz5 as S-acylation can affect protein turnover.[22] We used cycloheximide to block protein synthesis for different periods (0, 30, 60, 120 min) in NRK cells expressing *WT-Fz5-HA* or *3CS-Fz5-HA* (Figure S3D). Fz5 had a half-life of approximately 60 min, with no significant differences in degradation rate between WT-Fz5 and 3CS-Fz5 receptors (Figure S3E). Together, our results show that S-acylation does not affect Fz5 turnover but positively regulates the surface levels of this receptor by reducing its endocytosis.

Fz5 S-acylation regulates the canonical and divergent canonical Wnt pathways

Our findings that S-acylation deficiency reduced Fz5 surface levels thereby affecting its interaction with LRP6 and Dvl1 led us to examine downstream Wnt signaling. As Wnts promote presynaptic assembly through canonical Wnt signaling[5,7] (Figure 4A), we investigated this pathway by evaluating β-catenin levels (Figure 4B). *WT-Fz5-HA* expression led to a significant increase in the number of β-catenin puncta along axons compared with control hippocampal neurons (Figure 4C). In contrast, *3CS-Fz5-HA* expression did not increase β-catenin puncta (Figure 4C), indicating a deficiency in canonical Wnt signaling.

We also examined whether 3CS-Fz5 affects the divergent canonical Wnt pathway, which inhibits GSK3 but does not require β-catenin-mediated transcription.[53] In neurons, divergent canonical Wnt pathway activation promotes microtubule stability in axons[13] (Figure 4A). We therefore examined the levels of acetylated tubulin (Figure 4D), a marker of stable microtubules.[13,53] In differentiated NB2a neurons, expression of *WT-Fz5-HA* but not *3CS-Fz5-HA* significantly increased acetylated tubulin levels

(C) Diagram of Fz5-HA's transit through the endocytic pathway following antibody feeding. Colocalization of Fz5-HA with EEA1, Rab7, or Rab11 represented its presence at early, late, and recycling endosomes, respectively.

(D) Confocal images of WT-Fz5-HA or 3CS-Fz5-HA endocytic puncta colocalizing with endosomal markers (EAA1, Rab7, and Rab11). Fz5-HA (green), endosomal markers (red). Scale bars: 1 μm.

(E) Quantification of (D) for the number of WT-Fz5-HA or 3CS-Fz5-HA colocalized with each endocytic marker 15 min after antibody internalization (n = 20–25 cells, Mann-Whitney test [EEA1] or separate Student's t tests [Rab7 and Rab11]).

(F) Quantification of (D) for the percentage of WT-Fz5-HA or 3CS-Fz5-HA endocytic puncta colocalizing with endosomal markers 15 min after antibody internalization (n = 20–25 cells, Mann-Whitney test (EEA1) or separate Student's t tests [Rab7 and Rab11]).

Data expressed as mean ± SEM. Statistics: *p < 0.05, **p < 0.01, ***p < 0.001.

See also Figure S3.

Please cite this article in press as: Teo et al., S-acylation of the Wnt receptor Frizzled-5 by zDHHC5 controls its cellular localization and synaptogenic activity in the rodent hippocampus, Developmental Cell (2023), https://doi.org/10.1016/j.devcel.2023.07.012

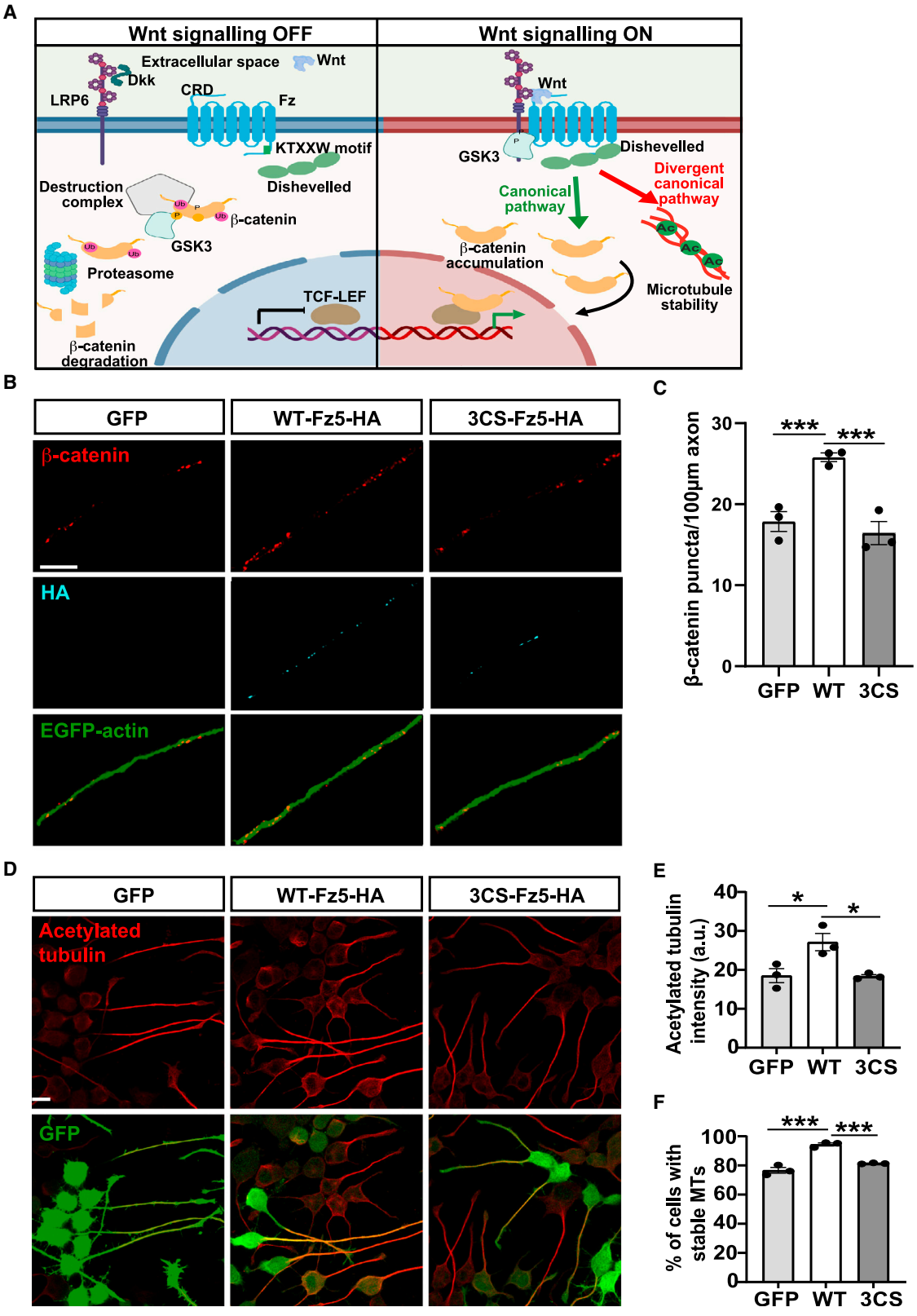

Figure 4. Fz5 S-acylation activates the canonical and divergent canonical Wnt pathways

(A) Diagram of canonical and divergent canonical Wnt signaling. In the absence of Wnts or presence of Wnt antagonist Dkk (Wnt signaling OFF), β-catenin is degraded. The multiprotein destruction complex includes GSK3. Wnt binding to Fz and co-receptor LRP6 (Wnt signaling ON) activates canonical signaling by

(legend continued on next page)

(Figure 4E) and the proportion of cells with stable microtubules (Figure 4F) when compared with control cells. Together, our results indicate that Fz5 S-acylation regulates both the canonical and divergent canonical Wnt pathways.

S-acylation promotes Fz5 localization to axons and presynaptic sites and is required for presynaptic assembly

We next investigated whether S-acylation affects Fz5 localization to different cellular compartments as this PTM can regulate protein trafficking.[22,54] We examined the localization of WT-Fz5 or 3CS-Fz5 in the soma, dendrites, or axons of hippocampal neurons (Figure S4A). The overall distribution of WT-Fz5 and 3CS-Fz5 was indistinguishable in the soma (Figure S4B). At dendrites, as previously reported,[21] Fz5 was localized along the dendritic shaft but not at dendritic spines (Figure S4C). Importantly, WT-Fz5 and 3CS-Fz5 exhibited the same dendritic distribution (Figure S4D). However, along the axon, the number of 3CS-Fz5 puncta was significantly lower compared with WT-Fz5, without changes in puncta volume (Figures 5A and 5B). Thus, Fz5 S-acylation is required for its localization along axons.

We also examined whether S-acylation affects Fz5 localization to presynaptic sites. To account for differences in the total levels of WT-Fz5 or 3CS-Fz5 along axons, we assessed the percentage (rather than absolute number) of Fz5-HA puncta that colocalized with the presynaptic marker vGlut1. The percentage of colocalized 3CS-Fz5 puncta was significantly lower than WT-Fz5 (Figures 5C and 5D). Thus, deficiency in S-acylation decreases Fz5 localization to axons and presynaptic sites.

We next evaluated whether S-acylation is required for Fz5-mediated synaptogenesis by evaluating the number of presynaptic vGlut1 sites along axons (Figure 5E). The number of vGlut1 puncta significantly increased with *WT-Fz5-HA* expression compared with *RFP*-expressing control neurons whereas *3CS-Fz5-HA* expression failed to change the number of vGlut1 puncta (Figure 5F). Thus, S-acylation is required for Fz5-mediated presynaptic assembly.

As shown above, *WT-Fz5* but not *3CS-Fz5* expression leads to β-catenin changes (Figures 4B and 4C), suggesting that canonical Wnt signaling is compromised when Fz5 is not S-acylated. Canonical Wnt signaling activation results in β-catenin translocation to the nucleus, which triggers TCF-dependent transcription (Figure 4A). To test whether Fz5 synaptogenic activity is mediated by canonical Wnt signaling, we expressed *WT-Fz5-HA* or *3CS-Fz5-HA* plus a dominant-negative mutant of TCF (TCFΔN) (Figure 5E), which blocks β-catenin-mediated transcription.[55] *TCFΔN* expression in neurons fully blocked the effect of WT-Fz5 on the number of vGlut1 puncta (Figure 5F). In contrast, *TCFΔN* expression did not affect the number of vGlut1 puncta in control neurons, or in neurons expressing *3CS-Fz5* (Figure 5F). These findings demonstrate that canonical Wnt signaling is required for Fz5-mediated presynaptic assembly and that deficiency in Fz5 S-acylation does not induce presynaptic assembly due to defects in canonical Wnt signaling.

Fz5 is S-acylated by the acyltransferase zDHHC5

How is Fz5 S-acylated? S-acylation is catalyzed by acyltransferases known as zinc-finger DHHCs (zDHHCs).[56] In mammals, there are at least 23 known members of this family, but zDHHC5 and zDHHC8 are the most highly expressed in the brain.[57] Thus, we focused on these two zDHHCs. We evaluated Fz5-HA S-acylation levels in HEK293 expressing *WT-Fz5-HA* or *3CS-Fz5-HA* in the presence or absence of *zDHHC5-myc* or *zDHHC8-myc* (Figure 6A). Expression of either *zDHHC5* or *zDHHC8* significantly increased WT-Fz5 S-acylation levels (Figure 6B). In contrast, neither *zDHHC5* nor *zDHHC8* expression changed 3CS-Fz5 S-acylation levels (Figure 6B). Thus, both zDHHC5 and zDHHC8 can S-acylate WT-Fz5.

To further elucidate the role of zDHHC5 and zDHHC8 in Fz5 S-acylation in neurons, we first investigated the localization of these enzymes in specific neuronal compartments. zDHHC8 does not localize to presynaptic sites,[58] where Fz5 receptors exert their synaptogenic effect,[20] but localizes to dendritic spines,[59] where Fz5 receptors are not enriched.[21] In contrast, zDHHC5 localizes to the dendritic shaft,[59] similar to Fz5.[21] However, the presence of zDHHC5 at presynaptic sites is unknown. To address this question, we isolated synaptosomes from mouse brains. Indeed, zDHHC5 was present in both the synaptosomal membrane fraction (SMF) and postsynaptic density (PSD) (Figure S5A). Together, these studies show that zDHHC5 and Fz5 are localized in the same neuronal compartments. Thus, we focused on zDHHC5 in subsequent experiments.

We performed zDHHC5 loss-of-function studies to evaluate its impact on endogenous Fz5 S-acylation. We utilized the CRISPR-Cas9 system to knockout endogenous zDHHC5 in hippocampal neurons (Figure S5B) by expressing a *Cas9* nuclease and a guide RNA (gRNA) against *zDHHC5* (Figure 6C). In zDHHC5 knockout neurons, endogenous Fz5 S-acylation was reduced by 50% compared with control levels (Figures 6D and 6E). Therefore, zDHHC5 is required for Fz5 S-acylation.

zDHHC5 knockout mimics the effect of S-acylation-deficient Fz5 receptor

To further confirm that zDHHC5 is required for Fz5 S-acylation, we investigated the effect of zDHHC5 knockout on WT-Fz5

recruiting Disheveled to the membrane and stabilizing β-catenin, which translocates to the nucleus to drive Wnt target gene expression through TCF/lymphoid enhancer binding factor (LEF). The divergent canonical pathway diverges downstream of GSK3 and regulates microtubule stability.

(B) Confocal images for β-catenin puncta along axons of hippocampal neurons expressing *EGFP-actin* only (control), or *EGFP-actin* and *WT-Fz5-HA* or *3CS-Fz5-HA*. EGFP-actin (green), β-catenin (red), and HA (cyan). Scale bars: 5 μm.

(C) Quantification of (B) for β-catenin puncta per 100 μm axon (n = 3 cultures, one-way ANOVA with Tukey's post hoc).

(D) Confocal images of differentiated NB2a cells expressing *GFP* only (control), or *GFP* with *WT-Fz5-HA* or *3CS-Fz5-HA*. GFP (green), acetylated tubulin (red). Scale bars: 14 μm.

(E) Quantification of (D) for acetylated tubulin intensity (n = 3 cultures, one-way ANOVA with Tukey's post hoc).

(F) Quantification of (D) for the percentage of cells with acetylated tubulin representing stable microtubules (n = 3 cultures, one-way ANOVA with Tukey's post hoc).

Data expressed as mean ± SEM. Statistics: *p < 0.05, ***p < 0.001.

Please cite this article in press as: Teo et al., S-acylation of the Wnt receptor Frizzled-5 by zDHHC5 controls its cellular localization and synaptogenic activity in the rodent hippocampus, Developmental Cell (2023), https://doi.org/10.1016/j.devcel.2023.07.012

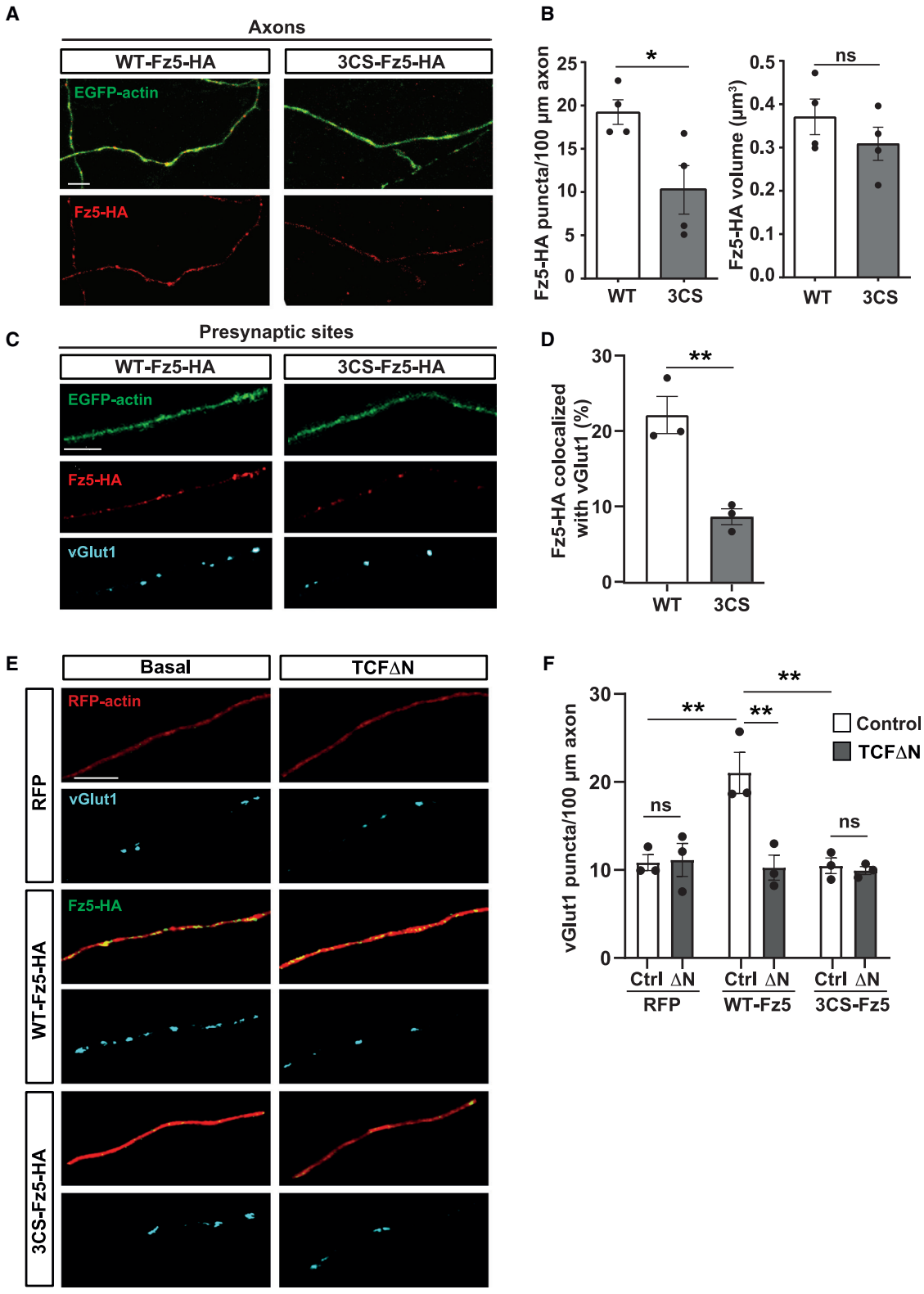

Figure 5. S-acylation regulates Fz5 localization to axons and to presynaptic sites and is required for Fz5 synaptogenic activity

(A) Confocal images of axons of hippocampal neurons expressing *EGFP-actin* and *WT-Fz5-HA* or *3CS-Fz5-HA*. EGFP-actin (green), HA (red). Scale bars: 5 µm.
(B) Quantification of (A) for the puncta number and volume of Fz5-HA (n = 4 cultures, Student's t test).

(legend continued on next page)

Please cite this article in press as: Teo et al., S-acylation of the Wnt receptor Frizzled-5 by zDHHC5 controls its cellular localization and synaptogenic activity in the rodent hippocampus, Developmental Cell (2023), https://doi.org/10.1016/j.devcel.2023.07.012

localization and function. We first analyzed the impact of zDHHC5 knockout on Fz5 surface localization using surface biotinylation experiments (Figure 6F). zDHHC5 knockout almost completely abolished endogenous Fz5 surface levels in hippocampal neurons without affecting total Fz5 levels (Figure 6G). Thus, zDHHC5 is required for Fz5 surface localization.

Next, we examined the impact of zDHHC5 knockout on Fz5 localization along axons. We expressed *WT-Fz5-HA* or *3CS-Fz5-HA* in hippocampal neurons where zDHHC5 has been knocked out (Figure 6C). zDHHC5 knockout significantly decreased WT-Fz5 axonal localization (Figures 6H and 6I). In contrast, zDHHC5 knockout had no effect on 3CS-Fz5 localization, consistent with the fact that 3CS-Fz5 is S-acylation deficient (Figures 6H and 6I). Thus, zDHHC5 knockout resulted in a similar number of WT-Fz5 and 3CS-Fz5 puncta along axons (Figures 6H and 6I). Therefore, zDHHC5 is required for WT-Fz5 receptor localization along axons.

We also examined the effect of zDHHC5 knockout on Fz5-mediated presynaptic assembly. Consistent with our previous results (Figures 5E and 5F), expression of *WT-Fz5-HA* but not *3CS-Fz5-HA* increased the number of presynaptic vGlut1 puncta in control neurons (no zDHHC5 knockout) (Figures 6H and 6J). With zDHHC5 knockout, the number of vGlut1 puncta decreased in *RFP*-, *WT-Fz5*-, and *3CS-Fz5*-expressing neurons (Figures 6H–6J), suggesting that zDHHC5 targets proteins that affect synapse formation.[60] Importantly, zDHHC5 knockout completely abolished the increase in presynaptic sites induced by *WT-Fz5* expression (Figures 6H–6J). Thus, the number of vGlut1 puncta was similar in *WT-Fz5*-expressing neurons when compared with *3CS-Fz5*-expressing neurons when zDHHC5 was knocked out (Figures 6H–6J). Our results establish that zDHHC5 is necessary for Fz5 presynaptic function and that WT-Fz5 behaves in an S-acylation-deficient manner when zDHHC5 is knocked out.

Fz5 S-acylation is regulated by neuronal activity and is required for activity-mediated presynaptic assembly

Our previous studies showed that the surface and synaptic levels of Fz5 receptors are regulated by the pattern of neuronal activity.[20] We therefore investigated whether neuronal activity regulates Fz5 S-acylation by inducing chemical long-term potentiation (cLTP) and chemical long-term depression (cLTD) (Figure 7A). cLTP increased the endogenous levels of S-acylated Fz5 in hippocampal neurons, whereas cLTD decreased S-acylated Fz5 levels (Figure 7B). Thus, the levels of S-acylated Fz5 are regulated by the pattern of neuronal activity.

Next, we examined whether neuronal activity regulates Fz5 S-acylation *in vivo* by exposing mice to an enriched environment (EE) (Figure 7C), a paradigm that elicits synapse formation in a Wnt-dependent manner.[61] Endogenous Fz5 S-acylation levels increased by 2-fold in the hippocampus following exposure to EE (Figure 7D). These results demonstrate that neuronal activity regulates endogenous Fz5 S-acylation.

Activity-mediated localization of Fz5 to the cell surface requires endogenous Wnts.[20] In particular, the levels of Wnt7a, which is a ligand of Fz5, increase with both HFS[21] and EE[61] (Figures S6A and S6B). Therefore, we evaluated whether Wnt7a enhances Fz5 S-acylation. S-acylated endogenous Fz5 levels significantly increased in hippocampal neurons after 3-h Wnt7a treatment compared with control neurons (Figures S6C and S6D). These results suggest that neuronal activity may promote Fz5 S-acylation through increased levels of Wnt7a.

Wnt7a-Fz5 signaling is required for activity-mediated synapse formation.[20] To address whether Fz5 S-acylation is required for this process, we used HFS to regulate neuronal activity[20] (Figure 7E). We compared the number of presynaptic terminals in unstimulated control versus HFS-stimulated hippocampal neurons (Figure 7F). In both control and *WT-Fz5-HA*-expressing neurons, HFS induced a significant increase in the number of vGlut1 puncta when compared with basal conditions (Figure 7G). However, HFS failed to increase the number of vGlut1 puncta in *3CS-Fz5-HA*-expressing neurons (Figure 7G). Thus, Fz5 S-acylation is required for activity-dependent presynaptic assembly.

S-acylation is required for *in vivo* Fz5-mediated presynaptic assembly

We then asked whether S-acylation is necessary for Fz5 function in the rodent hippocampus. To address this question, we injected adeno-associated virus-9 (AAV9) expressing *EGFP* only, *EGFP* and *WT-Fz5*, or *EGFP* and *3CS-Fz5* into the lateral ventricles of P0 and P1 WT mice (Figure 7H). We first examined whether the AAV injections of different Fz5 constructs changed hippocampal anatomy after 14 days of expression. DAPI staining showed no obvious differences in gross hippocampal anatomy between animals injected with PBS or with AAV9 (EGFP control, WT-Fz5 or 3CS-Fz5) (Figure S7A). Given that AAV injections into the brain could elicit neuroinflammation,[62] we also examined possible changes in astrocytes (glial fibrillary acidic protein [GFAP]-positive) and microglia (Iba1-positive), which increase during inflammation. However, no obvious differences were detected (Figure S7B). Thus, AAV injection and expression of *WT-Fz5* or *3CS-Fz5* in the hippocampus neither affects its overall development nor glial cell proliferation.

Next, we evaluated the *in vivo* effect of WT-Fz5 and 3CS-Fz5 receptors on presynaptic assembly at the peak of synaptogenesis (P14) (Figure 7H). We examined the stratum lacunosum moleculare (SLM), where highly infected principal neurons in the upper layers of the entorhinal cortex (Figure S7C) projected to and made synapses onto dendrites of CA1 cells. Expression of *WT-Fz5* significantly increased the number of presynaptic bassoon puncta compared with controls (Figures 7I and 7J). In contrast, expression of *3CS-Fz5* completely failed to increase

(C) Confocal images of axons of hippocampal neurons expressing *EGFP-actin* and *WT-Fz5-HA* or *3CS-Fz5-HA* labeled with presynaptic marker vGlut1. EGFP-actin (green), HA (red), and vGlut1 (cyan). Scale bars: 5 μm.
(D) Quantification of (C) showing the percentage of Fz5-HA colocalizing with vGlut1 (n = 3 cultures, Student's t test).
(E) Confocal images of axons of hippocampal neurons expressing *RFP-actin* only, or *RFP-actin* with *WT-Fz5-HA* or *3CS-Fz5-HA*, labeled with vGlut1. Neurons either did not express (basal) or expressed a dominant-negative form of *TCF* (*TCFΔN*). RFP-actin (red), HA (green), and vGlut1 (cyan). Scale bars: 5 μm.
(F) Quantification of (E) for the number of vGlut1 puncta per 100 μm axon (n = 3 cultures, two-way ANOVA with Tukey's post hoc).
Data expressed as mean ± SEM. Statistics: *p < 0.05, **p < 0.01.
See also Figure S4.

Please cite this article in press as: Teo et al., S-acylation of the Wnt receptor Frizzled-5 by zDHHC5 controls its cellular localization and synaptogenic activity in the rodent hippocampus, Developmental Cell (2023), https://doi.org/10.1016/j.devcel.2023.07.012

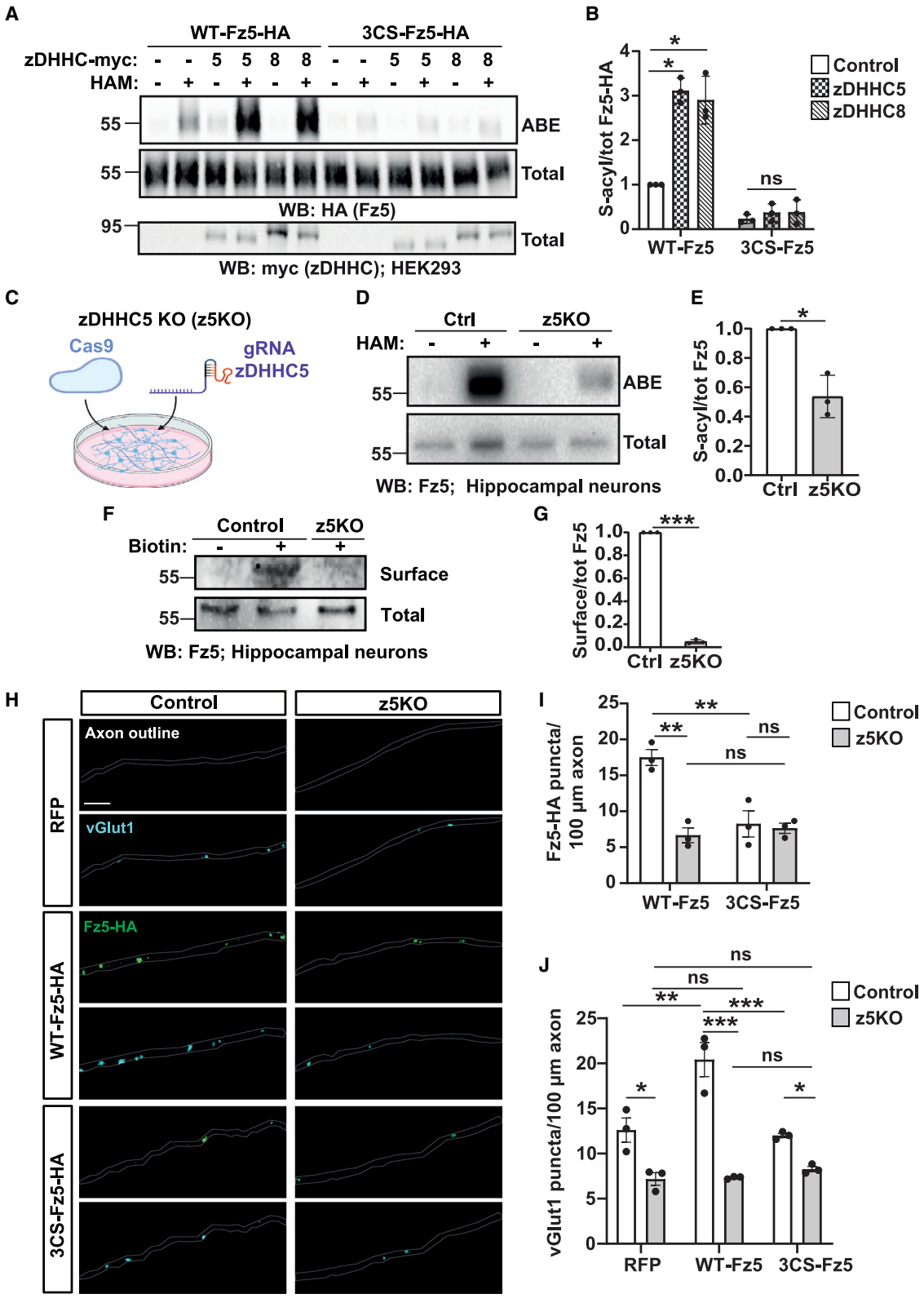

Figure 6. zDHHC5 is required for Fz5 S-acylation, its localization to the surface and along axons, and Fz5-mediated presynaptic assembly

(A) ABE assays from HEK293 expressing *WT-Fz5-HA* or *3CS-Fz5-HA* alone, or *Fz5-HA* plus *zDHHC5-myc*, or *Fz5-HA* plus *zDHHC8-myc*. Total levels of zDHHC-myc are shown to demonstrate the expression of these enzymes.

(legend continued on next page)

Please cite this article in press as: Teo et al., S-acylation of the Wnt receptor Frizzled-5 by zDHHC5 controls its cellular localization and synaptogenic activity in the rodent hippocampus, Developmental Cell (2023), https://doi.org/10.1016/j.devcel.2023.07.012

the number of bassoon puncta (Figures 7I and 7J). Therefore, Fz5 promotes presynaptic assembly in the developing hippocampus and S-acylation is required for this process.

DISCUSSION

Elucidating the molecular mechanisms that regulate membrane receptor localization and function is essential for understanding how extracellular proteins activate signaling pathways in different cellular compartments. Here, we demonstrate that Fz receptors are S-acylated. Although other Wnt signaling components such as LRP6 are known to be S-acylated,[63] we focus our attention on Fz5, which is required for Wnt-mediated presynaptic formation.[20] We demonstrate that Fz5 S-acylation is increased by neuronal activity and by Wnt7a. We also show that Fz5 S-acylation is required for presynaptic assembly, thus unraveling a mechanism through which this lipid modification in Wnt receptors regulates neuronal connectivity.

We demonstrate that all Fz receptors are predicted to be S-acylated on at least one cysteine residue in the transmembrane region or intracellularly, where S-acylation is typically thought to occur at these residues. Interestingly, the highest S-acylation prediction scores (>0.9) for some Fz receptors including Fz1-4 and Fz7 are for extracellular N-terminal residues. To our knowledge, the only receptor described to be S-acylated extracellularly is the amyloid precursor protein (APP).[64] Future studies will determine the region in which S-acylation occurs on Fz receptors other than Fz5.

Using three different approaches, we demonstrate Fz5 S-acylation. This PTM occurs endogenously in the brain and intestines, where Fz5 is highly expressed. Importantly, mutagenesis of three Fz5 C-terminal cysteines almost completely abolishes its S-acylation. Further evidence of Fz5 S-acylation comes from the identification of the enzyme involved in this process. zDHHC5 localizes to similar cellular compartments as Fz5. Importantly, loss-of-function studies in neurons using the CRISPR-Cas9 system demonstrate that zDHHC5 is required for Fz5 S-acylation.

What is the role of Fz5 S-acylation? Our studies revealed that this PTM is required for Fz5 surface localization as approximately 40% less of the 3CS-Fz5 mutant is present at the cell surface than the WT-Fz5 receptor. Decreased levels of surface 3CS-Fz5 are due to increased endocytosis. These results demonstrate that Fz5 S-acylation stabilizes this receptor at the cell surface.

The role of receptor endocytosis in Wnt signaling is complex. In the case of Fz5, its S-acylation stabilizes its surface levels by reducing endocytosis. Consistent with this finding, we observed a reduced interaction between 3CS-Fz5 and LRP6 or 3CS-Fz5 and Dvl1 compared with WT-Fz5 and LRP6 or WT-Fz5 and Dvl1. 3CS-Fz5 also fails to respond to Wnt7a by forming a complex with LRP6 and does not increase β-catenin puncta and microtubule stability, readouts of the canonical and divergent canonical Wnt pathways, respectively. Thus, S-acylation regulates Fz5 endocytosis and therefore its surface levels, resulting in a significant impact on receptor complex formation and downstream signaling.

Our studies also demonstrate that S-acylation is essential for Fz5 localization in axons. Expression of S-acylation-deficient Fz5 results in fewer Fz5 clusters along axons, whereas normal clustering and retention of S-acylation-deficient Fz5 occur at dendrites. Consistently, zDHHC5 knockout significantly decreases WT Fz5 axonal levels. This phenotype could be due to polarized sorting, retention, or clustering of the receptor.[54,65] Together, our findings demonstrate that S-acylation regulates Fz5 surface and axonal levels and suggest that Fz5 S-acylation is required for polarized trafficking to axons.

Does S-acylation affect Fz5-mediated presynaptic assembly? Gain of function of WT-Fz5 receptors promotes the formation of presynaptic sites whereas zDHHC5 knockout in neurons abolishes this effect. Consistently, expression of the S-acylation-deficient Fz5 mutant fails to promote presynaptic assembly in hippocampal neurons and in the developing mouse hippocampus. Thus, S-acylation is essential for Fz5 presynaptic function *in vitro* and *in vivo*. 3CS-Fz5 also blocks activity-mediated synapse assembly, an effect that could be due to the formation of non-functional heterodimers between mutant 3CS-Fz5 and WT-Fz5 receptors. Alternatively, 3CS-Fz5 might sequester Wnts, which could prevent the formation of receptor complexes required for downstream signaling. Therefore, Fz5 S-acylation is required for its presynaptic function both basally and in activity-mediated synapse assembly.

Here, we demonstrate that endogenous Fz receptors are S-acylated. Importantly, this PTM is regulated by neuronal activity and is required for Fz5 surface localization and function in

(B) Quantification of (A) for Fz5-HA S-acylation normalized to HEK293 expressing *WT-Fz5-HA* only (n = 3 cultures, two-way ANOVA with Games-Howell post hoc test).
(C) Schematic diagram of zDHHC5 knockout (z5KO) in hippocampal neurons. Cas9 and a guide RNA (gRNA) against zDHHC5 were co-transfected into neurons.
(D) ABE assays of endogenous Fz5 S-acylation levels in control or z5KO hippocampal neurons.
(E) Quantification of (D) for endogenous Fz5 S-acylation levels z5KO hippocampal neurons normalized to levels in control neurons (n = 3 cultures, one-sample t test).
(F) Endogenous Fz5 surface levels using biotinylation analyses in control or z5KO hippocampal neurons.
(G) Quantification of (F) for endogenous Fz5 surface levels in z5KO hippocampal neurons normalized to control levels (n = 3 cultures, one-sample t test).
(H) Confocal images of axons of control or z5KO hippocampal neurons expressing *RFP-actin* only, or *RFP-actin* with *WT-Fz5-HA* or *3CS-Fz5-HA*, labeled with the presynaptic marker vGlut1. Outline of *RFP-actin*-expressing axon (white lines), HA (green), vGlut1 (cyan). Scale bars: 5 μm.
(I) Quantification of (H) for number of Fz5-HA puncta per 100 μm axon (n = 3 cultures, two-way ANOVA with Tukey's post hoc).
(J) Quantification of (H) for the number of vGlut1 puncta per 100 μm axon (n = 3 cultures, two-way ANOVA with Tukey's post hoc).
For (A) and (D), samples were treated with hydroxylamine (+HAM) or vehicle control (negative controls, −HAM).
For (F), samples were treated with (+biotin) or without (negative controls, −biotin) sulfo-NHS-biotin for surface biotinylation assays.
Molecular weights (kDa) are indicated on the left of membranes.
Data expressed as mean ± SD (B, E, and G) or mean ± SEM (I and J). Statistics: *p < 0.05, **p < 0.01, ***p < 0.001.
See also Figure S5.

Please cite this article in press as: Teo et al., S-acylation of the Wnt receptor Frizzled-5 by zDHHC5 controls its cellular localization and synaptogenic activity in the rodent hippocampus, Developmental Cell (2023), https://doi.org/10.1016/j.devcel.2023.07.012

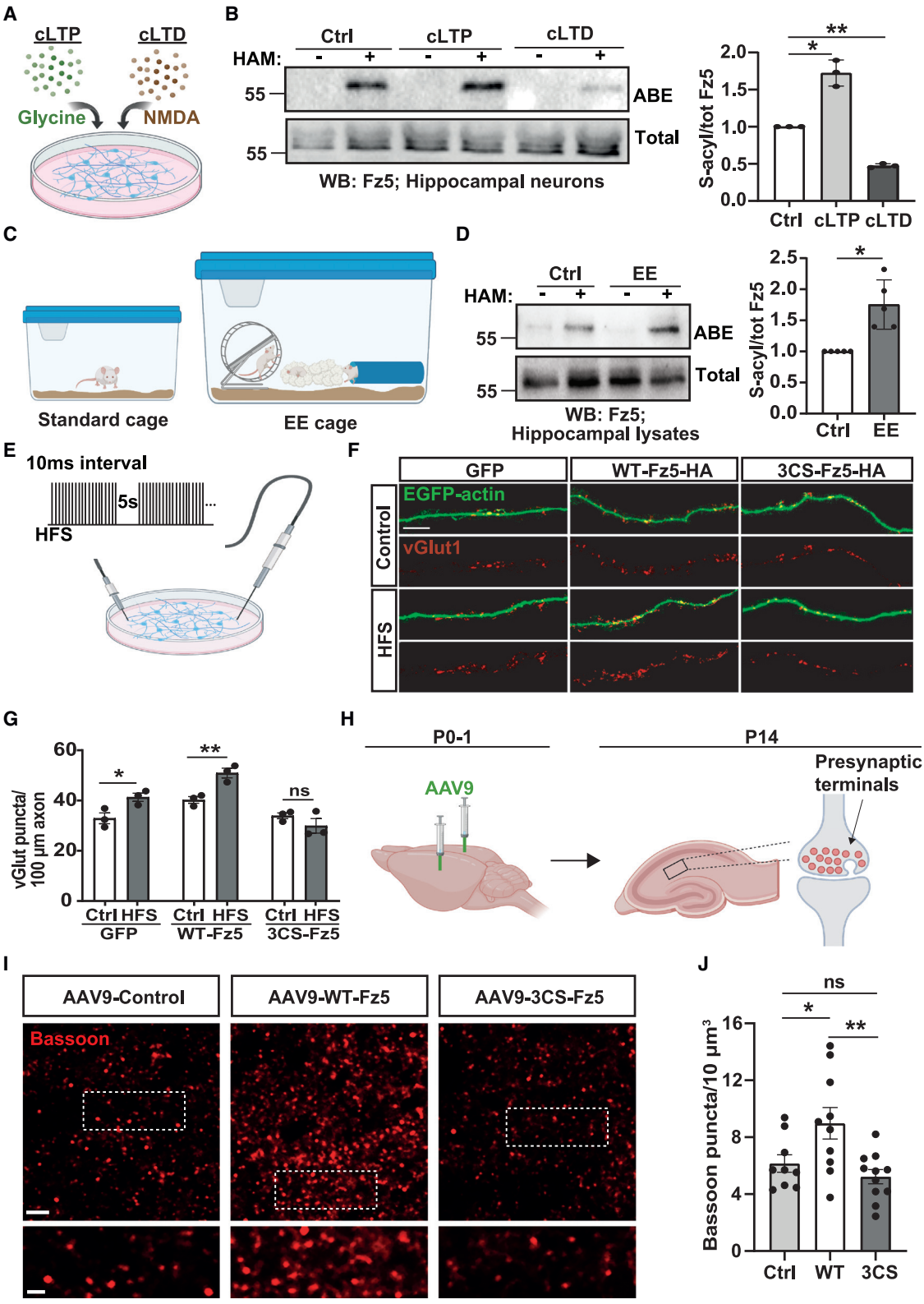

Figure 7. Neuronal activity regulates Fz5 S-acylation, which is required for *in vivo* and activity-mediated presynaptic assembly

(A) Diagram showing chemical long-term potentiation (cLTP) and chemical long-term depression (cLTD) induction in hippocampal neurons using glycine or N-methyl-D-aspartate (NMDA), respectively.

(B) ABE assays from hippocampal neurons exposed to basal control, cLTP or cLTD. (n = 3 cultures, Kruskal-Wallis with Games-Howell post hoc test.)

(legend continued on next page)

synapse assembly. Our data shed light on the role of Fz receptor S-acylation in regulating their cellular localization and function. Our results provide increased avenues to explore how Fz function is regulated in health and disease.

Limitations of the study

To study Fz5 S-acylation, we overexpressed WT-Fz5 and 3CS-Fz5 receptors. Although these were not endogenous 3CS-Fz5 studies, the results obtained were consistent with those from the knockout of endogenous zDHHC5, the enzyme required for Fz5 S-acylation. Indeed, zDHHC5 knockout in neurons mimics the effect of 3CS-Fz5 overexpression. For future studies, the generation of endogenous 3CS mutant cells will provide a valuable tool to study the impact of Fz5 S-acylation.

Although endogenous zDHHC5 knockout completely abolishes Fz5-mediated presynaptic assembly, it only decreases Fz5 S-acylation by 50%. These results suggest that other enzymes might also S-acylate Fz5.

STAR★METHODS

Detailed methods are provided in the online version of this paper and include the following:

SUPPLEMENTAL INFORMATION

Supplemental information can be found online at https://doi.org/10.1016/j.devcel.2023.07.012.

ACKNOWLEDGMENTS

We thank M. Sahores for some preliminary results and M. Skehel, T. Auchynnikava, and members of our laboratory for useful discussions. We also thank H. Clevers, Y. Goda, X. He, B. Holdener, A. Kihara, E. Metzakopian, and G. Wayman for DNA constructs. CMA was a gift from B. Dickinson. Illustrations were created with BioRender.com.

This work was supported by the BBSRC (BB/S016104/1), the MRC (MR/S012125/1, MC_ST_U14006, and MC_ST_U15013), and Alzheimer's Research UK (ARUK-IRG2016A-7 and ARUK-PPG2021B-030).

AUTHOR CONTRIBUTIONS

Conceptualization, P.C.S.; methodology, S.T., A.B., E.S., and P.C.S.; investigation, S.T., A.B., E.S., P.P.-V., and M.E.J.; resources, L.-N.S.; writing—riginal draft, A.B., E.S., and P.C.S.; writing—review and editing, S.T. and P.C.S.; supervision, P.C.S.; funding acquisition, P.C.S.

DECLARATION OF INTERESTS

The authors declare no competing interests.

Received: September 16, 2022
Revised: May 5, 2023
Accepted: July 18, 2023
Published: October 23, 2023

(C) Diagram showing a mouse in a standard cage versus mice exposed to an enriched environment (EE).
(D) ABE assays from mouse hippocampi exposed to control standard housing or EE. (n = 4 animals, one-sample t test.)
For (B) and (D), samples were treated with hydroxylamine (+HAM) or vehicle control (negative controls, −HAM). Molecular weights (kDa) are indicated on the left of membranes.
(E) Diagram showing high-frequency stimulation (HFS) in hippocampal neurons. A regular stimulation pattern was delivered with 5 s between trains.
(F) Confocal images of axons of hippocampal neurons expressing *EGFP-actin* only (control), or *EGFP-actin* with *WT-Fz5-HA* or *3CS-Fz5-HA* exposed to basal (control) or HFS conditions. Neurons were labeled with the presynaptic marker vGlut1. EGFP-actin (green), vGlut1 (red). Scale bars: 8 μm.
(G) Quantification of (F) for the number of vGlut1 puncta per 100 μm axon (n = 3 cultures, two-way ANOVA with Bonferroni post hoc).
(H) Schematic diagram showing AAV9 injection into lateral ventricles of each hemisphere of P0 and P1 mice. At P14, the density of presynaptic terminals was analyzed in the stratum lacunosum moleculare (SLM, box).
(I) Confocal images of the SLM of mice injected with AAV9-control, WT-Fz5, or 3CS-Fz5. Bassoon (presynaptic marker, red). Scale bars: 2.5 μm (top) and 1 μm (bottom).
(J) Quantification of (I) of the number of bassoon puncta (n = 9 control, 10 WT-Fz5, 11 3CS-Fz5 animals, one-way ANOVA with Tukey's post hoc).
Data expressed as mean ± SD (B and D) or mean ± SEM (G and J). Statistics: *$p < 0.05$, **$p < 0.01$, ***$p < 0.001$.
See also Figures S6 and S7.

REFERENCES

1. Mizumoto, K., Jin, Y., and Bessereau, J.L. (2023). Synaptogenesis: unmasking molecular mechanisms using Caenorhabditis elegans. Genetics *223*, iyac176.
2. Südhof, T.C. (2021). The cell biology of synapse formation. J. Cell Biol. *220*, e202103052.
3. Favuzzi, E., and Rico, B. (2018). Molecular diversity underlying cortical excitatory and inhibitory synapse development. Curr. Opin. Neurobiol. *53*, 8–15.
4. Teo, S., and Salinas, P.C. (2021). Wnt-Frizzled signaling regulates activity-mediated synapse formation. Front. Mol. Neurosci. *14*, 683035.
5. Budnik, V., and Salinas, P.C. (2011). Wnt signaling during synaptic development and plasticity. Curr. Opin. Neurobiol. *21*, 151–159.
6. Feng, B., Freitas, A.E., Gorodetski, L., Wang, J., Tian, R., Lee, Y.R., Grewal, A.S., and Zou, Y. (2021). Planar cell polarity signaling components are a direct target of β-amyloid-associated degeneration of glutamatergic synapses. Sci. Adv. *7*, eabh2307.
7. Park, M., and Shen, K. (2012). WNTs in synapse formation and neuronal circuitry. EMBO J. *31*, 2697–2704.
8. Schulte, G. (2010). International union of basic and Clinical Pharmacology. LXXX. The class Frizzled receptors. Pharmacol. Rev. *62*, 632–667.
9. Wang, Y., Chang, H., Rattner, A., and Nathans, J. (2016). Frizzled receptors in development and disease. Curr. Top. Dev. Biol. *117*, 113–139.
10. Rim, E.Y., Clevers, H., and Nusse, R. (2022). The Wnt pathway: from signaling mechanisms to synthetic modulators. Annu. Rev. Biochem. *91*, 571–598.
11. Nusse, R., and Clevers, H. (2017). Wnt/β-Catenin signaling, disease, and emerging therapeutic modalities. Cell *169*, 985–999.
12. Wiese, K.E., Nusse, R., and van Amerongen, R. (2018). Wnt signalling: conquering complexity. Development *145*, dev165902.
13. Ciani, L., Krylova, O., Smalley, M.J., Dale, T.C., and Salinas, P.C. (2004). A divergent canonical WNT-signaling pathway regulates microtubule dynamics: dishevelled signals locally to stabilize microtubules. J. Cell Biol. *164*, 243–253.
14. Devenport, D. (2014). The cell biology of planar cell polarity. J. Cell Biol. *207*, 171–179.
15. Gray, R.S., Roszko, I., and Solnica-Krezel, L. (2011). Planar cell polarity: coordinating morphogenetic cell behaviors with embryonic polarity. Dev. Cell *21*, 120–133.
16. He, C.W., Liao, C.P., and Pan, C.L. (2018). Wnt signalling in the development of axon, dendrites and synapses. Open Biol. *8*, 180116.
17. Stoeckli, E.T. (2018). Understanding axon guidance: are we nearly there yet? Development *145*, dev151415.
18. McLeod, F., and Salinas, P.C. (2018). Wnt proteins as modulators of synaptic plasticity. Curr. Opin. Neurobiol. *53*, 90–95.
19. Ferrari, M.E., Bernis, M.E., McLeod, F., Podpolny, M., Coullery, R.P., Casadei, I.M., Salinas, P.C., and Rosso, S.B. (2018). Wnt7b signalling through Frizzled-7 receptor promotes dendrite development by coactivating CaMKII and JNK. J. Cell Sci. *131*, jcs216101.
20. Sahores, M., Gibb, A., and Salinas, P.C. (2010). Frizzled-5, a receptor for the synaptic organizer Wnt7a, regulates activity-mediated synaptogenesis. Development *137*, 2215–2225.
21. McLeod, F., Bossio, A., Marzo, A., Ciani, L., Sibilla, S., Hannan, S., Wilson, G.A., Palomer, E., Smart, T.G., Gibb, A., et al. (2018). Wnt signaling mediates LTP-dependent spine plasticity and AMPAR localization through Frizzled-7 receptors. Cell Rep. *23*, 1060–1071.
22. Linder, M.E., and Deschenes, R.J. (2007). Palmitoylation: policing protein stability and traffic. Nat. Rev. Mol. Cell Biol. *8*, 74–84.
23. Resh, M.D. (2013). Covalent lipid modifications of proteins. Curr. Biol. *23*, R431–R435.
24. Chamberlain, L.H., and Shipston, M.J. (2015). The physiology of Protein S-acylation. Physiol. Rev. *95*, 341–376.
25. Percherancier, Y., Planchenault, T., Valenzuela-Fernandez, A., Virelizier, J.L., Arenzana-Seisdedos, F., and Bachelerie, F. (2001). Palmitoylation-dependent control of degradation, life span, and membrane expression of the CCR5 receptor. J. Biol. Chem. *276*, 31936–31944.
26. Roberts, B.J., Svoboda, R.A., Overmiller, A.M., Lewis, J.D., Kowalczyk, A.P., Mahoney, M.G., Johnson, K.R., and Wahl, J.K. (2016). Palmitoylation of Desmoglein 2 is a regulator of assembly dynamics and protein turnover. J. Biol. Chem. *291*, 24857–24865.
27. Ernst, A.M., Syed, S.A., Zaki, O., Bottanelli, F., Zheng, H., Hacke, M., Xi, Z., Rivera-Molina, F., Graham, M., Rebane, A.A., et al. (2018). S-Palmitoylation sorts membrane cargo for anterograde transport in the Golgi. Dev. Cell *47*, 479–493.e7.
28. Salaun, C., Greaves, J., and Chamberlain, L.H. (2010). The intracellular dynamic of protein palmitoylation. J. Cell Biol. *191*, 1229–1238.
29. Charollais, J., and Van Der Goot, F.G. (2009). Palmitoylation of membrane proteins (Review). Mol. Membr. Biol. *26*, 55–66.
30. Sanders, S.S., Martin, D.D.O., Butland, S.L., Lavallée-Adam, M., Calzolari, D., Kay, C., Yates, J.R., and Hayden, M.R. (2015). Curation of the mammalian palmitoylome indicates a pivotal role for palmitoylation in diseases and disorders of the nervous system and cancers. PLoS Comput. Biol. *11*, e1004405.
31. Cho, E., and Park, M. (2016). Palmitoylation in Alzheimer's disease and other neurodegenerative diseases. Pharmacol. Res. *111*, 133–151.
32. Kang, R., Wan, J., Arstikaitis, P., Takahashi, H., Huang, K., Bailey, A.O., Thompson, J.X., Roth, A.F., Drisdel, R.C., Mastro, R., et al. (2008). Neural palmitoyl-proteomics reveals dynamic synaptic palmitoylation. Nature *456*, 904–909.
33. Ning, W., Jiang, P., Guo, Y., Wang, C., Tan, X., Zhang, W., Peng, D., and Xue, Y. (2021). GPS-Palm: a deep learning-based graphic presentation system for the prediction of S-palmitoylation sites in proteins. Brief. Bioinform. *22*, 1836–1847.
34. Ramírez, V.T., Ramos-Fernández, E., Henríquez, J.P., Lorenzo, A., and Inestrosa, N.C. (2016). Wnt-5a/frizzled9 receptor signaling through the Gαo-Gβγ complex regulates dendritic spine formation. J. Biol. Chem. *291*, 19092–19107.
35. Fukata, M., Fukata, Y., Adesnik, H., Nicoll, R.A., and Bredt, D.S. (2004). Identification of PSD-95 palmitoylating enzymes. Neuron *44*, 987–996.
36. Hayashi, T., Rumbaugh, G., and Huganir, R.L. (2005). Differential regulation of AMPA receptor subunit trafficking by palmitoylation of two distinct sites. Neuron *47*, 709–723.
37. van Es, J.H., Jay, P., Gregorieff, A., van Gijn, M.E., Jonkheer, S., Hatzis, P., Thiele, A., van den Born, M., Begthel, H., Brabletz, T., et al. (2005). Wnt signalling induces maturation of Paneth cells in intestinal crypts. Nat. Cell Biol. *7*, 381–386.
38. Nadolski, M.J., and Linder, M.E. (2007). Protein lipidation. FEBS Journal *274*, 5202–5210.
39. Davda, D., El Azzouny, M.A., Tom, C.T.M.B., Hernandez, J.L., Majmudar, J.D., Kennedy, R.T., and Martin, B.R. (2013). Profiling targets of the irreversible palmitoylation inhibitor 2-bromopalmitate. ACS Chem. Biol. *8*, 1912–1917.
40. Azizi, S.A., Lan, T., Delalande, C., Kathayat, R.S., Banales Mejia, F.B., Qin, A., Brookes, N., Sandoval, P.J., and Dickinson, B.C. (2021). Development of an acrylamide-based inhibitor of protein S-acylation. ACS Chem. Biol. *16*, 1546–1556.
41. Gao, C., and Chen, Y.G. (2010). Dishevelled: the hub of Wnt signaling. Cell. Signal. *22*, 717–727.
42. Tauriello, D.V.F., Jordens, I., Kirchner, K., Slootstra, J.W., Kruitwagen, T., Bouwman, B.A.M., Noutsou, M., Rüdiger, S.G.D., Schwamborn, K., Schambony, A., et al. (2012). Wnt/β-catenin signaling requires interaction of the Dishevelled DEP domain and C terminus with a discontinuous motif in Frizzled. Proc. Natl. Acad. Sci. USA *109*, E812–E820.
43. Nile, A.H., Mukund, S., Stanger, K., Wang, W., and Hannoush, R.N. (2017). Unsaturated fatty acyl recognition by Frizzled receptors mediates

dimerization upon Wnt ligand binding. Proc. Natl. Acad. Sci. USA *114*, 4147–4152.

44. DeBruine, Z.J., Ke, J., Harikumar, K.G., Gu, X., Borowsky, P., Williams, B.O., Xu, W., Miller, L.J., Xu, H.E., and Melcher, K. (2017). Wnt5a promotes Frizzled-4 signalosome assembly by stabilizing cysteine-rich domain dimerization. Genes Dev. *31*, 916–926.
45. Hua, Y., Yang, Y., Li, Q., He, X., Zhu, W., Wang, J., and Gan, X. (2018). Oligomerization of Frizzled and LRP5/6 protein initiates intracellular signaling for the canonical WNT/β-catenin pathway. J. Biol. Chem. *293*, 19710–19724.
46. Eubelen, M., Bostaille, N., Cabochette, P., Gauquier, A., Tebabi, P., Dumitru, A.C., Koehler, M., Gut, P., Alsteens, D., Stainier, D.Y.R., et al. (2018). A molecular mechanism for Wnt ligand-specific signaling. Science *361*, eaat1178.
47. Zeng, X., Huang, H., Tamai, K., Zhang, X., Harada, Y., Yokota, C., Almeida, K., Wang, J., Doble, B., Woodgett, J., et al. (2008). Initiation of Wnt signaling: control of Wnt coreceptor Lrp6 phosphorylation/activation via frizzled, dishevelled and axin functions. Development *135*, 367–375.
48. Goddard, A.D., and Watts, A. (2012). Regulation of G protein-coupled receptors by palmitoylation and cholesterol. BMC Biol. *10*, 27.
49. Naumenko, V.S., and Ponimaskin, E. (2018). Palmitoylation as a functional regulator of neurotransmitter receptors. Neural Plast. *2018*, 5701348.
50. Kim, S., Lee, B.C., Lee, A.R., Won, S., and Park, C.S. (2014). Effects of palmitoylation on the diffusional movement of BKCa channels in live cells. FEBS Lett. *588*, 713–719.
51. Miesenböck, G., De Angelis, D.A., and Rothman, J.E. (1998). Visualizing secretion and synaptic transmission with pH-sensitive green fluorescent proteins. Nature *394*, 192–195.
52. Hildick, K.L., González-González, I.M., Jaskolski, F., and Henley, J.M. (2012). Lateral diffusion and exocytosis of membrane proteins in cultured neurons assessed using fluorescence recovery and fluorescence-loss photobleaching. J. Vis. Exp. 3747.
53. Salinas, P.C. (2007). Modulation of the microtubule cytoskeleton: a role for a divergent canonical Wnt pathway. Trends Cell Biol. *17*, 333–342.
54. Fukata, Y., and Fukata, M. (2010). Protein palmitoylation in neuronal development and synaptic plasticity. Nat. Rev. Neurosci. *11*, 161–175.
55. Roose, J., Huls, G., Van Beest, M., Moerer, P., Van Der Horn, K., Goldschmeding, R., Logtenberg, T., and Clevers, H. (1999). Synergy between tumor suppressor APC and the beta-catenin-Tcf4 target Tcf1. Science *285*, 1923–1926.
56. Malgapo, M.I.P., and Linder, M.E. (2021). Substrate recruitment by zDHHC protein acyltransferases. Open Biol. *11*, 210026.
57. Trinidad, J.C., Thalhammer, A., Specht, C.G., Lynn, A.J., Baker, P.R., Schoepfer, R., and Burlingame, A.L. (2008). Quantitative analysis of synaptic phosphorylation and protein expression. Mol. Cell. Proteomics *7*, 684–696.
58. Yang, Q., Zheng, F., Hu, Y., Yang, Y., Li, Y., Chen, G., Wang, W., He, M., Zhou, R., Ma, Y., et al. (2018). ZDHHC8 critically regulates seizure susceptibility in epilepsy. Cell Death Dis. *9*, 795.
59. Thomas, G.M., Hayashi, T., Chiu, S.L., Chen, C.M., and Huganir, R.L. (2012). Palmitoylation by DHHC5/8 targets GRIP1 to dendritic endosomes to regulate AMPA-R trafficking. Neuron *73*, 482–496.
60. Shimell, J.J., Globa, A., Sepers, M.D., Wild, A.R., Matin, N., Raymond, L.A., and Bamji, S.X. (2021). Regulation of hippocampal excitatory synapses by the Zdhhc5 palmitoyl acyltransferase. J. Cell Sci. *134*, jcs254276.
61. Gogolla, N., Galimberti, I., Deguchi, Y., and Caroni, P. (2009). Wnt signaling mediates experience-related regulation of synapse numbers and mossy fiber connectivities in the adult hippocampus. Neuron *62*, 510–525.
62. Perez, B.A., Shutterly, A., Chan, Y.K., Byrne, B.J., and Corti, M. (2020). Management of neuroinflammatory responses to AAV-mediated gene therapies for neurodegenerative diseases. Brain Sci. *10*, 119.
63. Abrami, L., Kunz, B., Iacovache, I., and Van Der Goot, F.G. (2008). Palmitoylation and ubiquitination regulate exit of the Wnt signaling protein LRP6 from the endoplasmic reticulum. Proc. Natl. Acad. Sci. USA *105*, 5384–5389.
64. Bhattacharyya, R., Barren, C., and Kovacs, D.M. (2013). Palmitoylation of amyloid precursor protein regulates amyloidogenic processing in lipid rafts. J. Neurosci. *33*, 11169–11183.
65. Globa, A.K., and Bamji, S.X. (2017). Protein palmitoylation in the development and plasticity of neuronal connections. Curr. Opin. Neurobiol. *45*, 210–220.
66. Krylova, O., Messenger, M.J., and Salinas, P.C. (2000). Dishevelled-1 regulates microtubule stability: a new function mediated by glycogen synthase kinase-3beta. J. Cell Biol. *151*, 83–94.
67. Dotti, C.G., Sullivan, C.A., and Banker, G.A. (1988). The establishment of polarity by hippocampal neurons in culture. J. Neurosci. *8*, 1454–1468.
68. Kim, J.Y., Grunke, S.D., Levites, Y., Golde, T.E., and Jankowsky, J.L. (2014). Intracerebroventricular viral injection of the neonatal mouse brain for persistent and widespread neuronal transduction. J. Vis. Exp. 51863.
69. Kamal, A., Ramakers, G.M., Urban, I.J., De Graan, P.N., and Gispen, W.H. (1999). Chemical LTD in the CA1 field of the hippocampus from young and mature rats. Eur. J. Neurosci. *11*, 3512–3516.
70. Ahmad-Annuar, A., Ciani, L., Simeonidis, I., Herreros, J., Ben Fredj, N.B., Rosso, S.B., Hall, A., Brickley, S., and Salinas, P.C. (2006). Signaling across the synapse: a role for Wnt and Dishevelled in presynaptic assembly and neurotransmitter release. J. Cell Biol. *174*, 127–139.
71. Wan, J., Roth, A.F., Bailey, A.O., and Davis, N.G. (2007). Palmitoylated proteins: purification and identification. Nat. Protoc. *2*, 1573–1584.
72. Hannoush, R.N. (2012). Profiling cellular myristoylation and palmitoylation using ω-alkynyl fatty acids. Methods Mol. Biol. *800*, 85–94.
73. McLeod, F., Marzo, A., Podpolny, M., Galli, S., and Salinas, P. (2017). Evaluation of synapse density in hippocampal rodent brain slices. J. Vis. Exp.e56153

Please cite this article in press as: Teo et al., S-acylation of the Wnt receptor Frizzled-5 by zDHHC5 controls its cellular localization and synaptogenic activity in the rodent hippocampus, Developmental Cell (2023), https://doi.org/10.1016/j.devcel.2023.07.012

STAR★METHODS

KEY RESOURCES TABLE

REAGENT or RESOURCE	SOURCE	IDENTIFIER
Antibodies		
Rat monoclonal anti-HA	Roche	Cat# 11867423001 RRID: AB_390918
Mouse monoclonal anti-bassoon	Novus	Cat# NB120-13249 RRID: AB_788125
Chicken polyclonal anti-GFAP	Millipore	Cat# AB5541 RRID: AB_177521
Rabbit polyclonal anti-Iba1	Synaptic Systems	Cat# 234003 RRID: AB_10641962
Rabbit monoclonal anti-EEA1	Cell Signaling Technology	Cat# 3288 RRID: AB_2096811
Rabbit monoclonal anti-Rab11	Cell Signaling Technology	Cat# 5589 RRID: AB_10693925
Rabbit monoclonal anti-Rab7	Cell Signaling Technology	Cat# 9367 RRID: AB_1904103
Chicken polyclonal anti-GFP	Millipore	Cat# 06-896 RRID: AB_310288
Rabbit polyclonal anti-GFP	Thermo Fisher Scientific	Cat# A-6455 RRID: AB_221570
Guinea pig polyclonal anti-vGlut1	Millipore	Cat# AB5905 RRID: AB_2301751
Mouse monoclonal anti-acetylated tubulin	Sigma-Aldrich	Cat# T6793 RRID: AB_477585
Mouse monoclonal anti-Fz5	Sigma-Aldrich	Cat# WH0007855M1 RRID: AB_1841684
Rabbit polyclonal anti-Fz5	Millipore	Cat# 06-756 RRID: AB_2109366
Rabbit polyclonal anti-Homer1	Synaptic Systems	Cat# 160002 RRID: AB_2120990
Rabbit polyclonal anti-Synaptophysin1	Synaptic Systems	Cat# 101002 RRID: AB_887905
Rabbit monoclonal anti-GAPDH	Abcam	Cat# ab181602 RRID: AB_2630358
Rabbit monoclonal anti-GluA1	Cell Signaling Technology	Cat# 13185 RRID: AB_2732897
Mouse monoclonal anti-PSD95	Thermo Fisher Scientific	Cat# MA1-046 RRID: AB_2092361
Mouse monoclonal anti-vinculin	Sigma-Aldrich	Cat# V4505 RRID: AB_477617
Rabbit polyclonal anti-MAP Kinase (ERK)	Sigma-Aldrich	Cat# M5670 RRID: AB_477216
Goat polyclonal anti-Wnt7a/b	R&D Systems	Cat# AF3460 RRID: AB_2304437
Rabbit polyclonal anti-HA	Sigma-Aldrich	Cat# H6908 RRID: AB_260070
Rabbit monoclonal anti-LRP6	Cell Signaling Technology	Cat# 2560 RRID: AB_2139329
Mouse monoclonal anti-rhodopsin (1D4)	Thermo Fisher Scientific	Cat# MA1-722 RRID: AB_325050

(*Continued on next page*)

Please cite this article in press as: Teo et al., S-acylation of the Wnt receptor Frizzled-5 by zDHHC5 controls its cellular localization and synaptogenic activity in the rodent hippocampus, Developmental Cell (2023), https://doi.org/10.1016/j.devcel.2023.07.012

Continued

REAGENT or RESOURCE	SOURCE	IDENTIFIER
Mouse monoclonal anti-β-catenin	BD Biosciences	Cat# 610153 RRID: AB_397554
Rabbit polyclonal anti-Fz7	Origene	Cat# TA344065
Mouse polyclonal anti-Fz9	R&D Systems	Cat# AF2440 RRID: AB_2232061
Rabbit polyclonal anti-zDHHC5	Proteintech	Cat# 21324-1-AP RRID: AB_10732816
Mouse monoclonal anti-Myc	Thermo Fisher Scientific	Cat# MA1-21316 RRID: AB_558473
Rabbit polyclonal anti-mCherry	Abcam	Cat# ab167453 RRID: AB_2571870
Bacterial and virus strains		
Adeno-associated viruses serotype 9 (AAV9)	Vector Builder	Custom made
Chemicals, peptides, and recombinant proteins		
Cycloheximide (50 μg/ml)	Cell Signaling Technology	Cat# 2112
2-bromopalmitate (100 μM)	Sigma-Aldrich	Cat# 238422
Cyano-myracrylamide (20 μM)	Prof Bryan C. Dickinson, Univrsity of Chicago	N/A
Recombinant human Wnt7a (200 ng/ml)	PeproTech	Cat# 120-31
N6,2'-O-Dibutyryladenosine 3',5'-cyclic monophosphate sodium salt (1 mM)	Sigma-Aldrich	Cat# D0627
N-ethylmaleimide (NEM, 10 mM)	Pierce	Cat# 23030
Hydroxylamine hydrochloride (10 mM)	Sigma-Aldrich	Cat# 255580
^{3}H palmitate (1 mCi/ml)	NEN Radiochemicals	Cat# NET043001MC
DAPI solution (1 mg/ml)	Thermo Fischer Scientific	Cat# 62248
Palmitic Acid Alkyne (100 μM)	Cayman Chemical	Cat# 13266
Bovine Serum Albumin, fatty acid free (5% w/v)	Sigma-Aldrich	Cat# A8806
Biotin Azide (100 μM)	Thermo Fischer Scientific	Cat# B10184
NMDA (50 μM)	Tocris Bioscience	Cat# 0114
Glycine (200 μM)	Thermo Fischer Scientific	Cat# 220910050
Terodotoxin citrate (0.5 μM)	Hellobio	Cat# HB10356
Strychnine (3 μM)	Thermo Fischer Scientific	Cat# 158950250
Bicuculline (20 μM)	Cayman Chemical	Cat# CAY11727
D-AP5 (20 μM)	Cayman Chemical	Cat# CAY14539
Phenylmethanesulfonyl fluoride (2 mM)	Sigma-Aldrich	Cat# P7626
Chymostatin (10-25 μg/ml)	Sigma-Aldrich	Cat# C7268
Leupeptin (10-25 μg/ml)	Sigma-Aldrich	Cat# L2884
Antipain (10-25 μg/ml)	Sigma-Aldrich	Cat# 10791
Pepstatin A (10-25 μg/ml)	Sigma-Aldrich	Cat# 77170
N^{α}-tosyl-lys Chloromethyl Ketone (10 μg/ml)	Sigma-Aldrich	Cat# 616382
Phosphatase Inhibitor Cocktail 2 (1X)	Sigma-Aldrich	Cat# P5726
cOmplete Protease Inhibitor Cocktail (1X)	Roche	Cat# 04693132001
N-2 Supplement (1X)	Gibco	Cat# 17502048
B-27 Supplement (1X)	Gibco	Cat# 17504044
L-glutamine (1 mM)	Gibco	Cat# 25030081
Glucose (10 mM)	Gibco	Cat# A2494001
Penicillin-Streptomycin (1% v/v)	Gibco	Cat# 15140122
Fetal Bovine Serum (10% v/v)	Gibco	Cat# 16000044
Critical commercial assays		
QuikChange Lightning Site-Directed Mutagenesis kit (for cloning of 3CS-Fz5)	Agilent Technologies	Cat# 210518

(*Continued on next page*)

Please cite this article in press as: Teo et al., S-acylation of the Wnt receptor Frizzled-5 by zDHHC5 controls its cellular localization and synaptogenic activity in the rodent hippocampus, Developmental Cell (2023), https://doi.org/10.1016/j.devcel.2023.07.012

Continued

REAGENT or RESOURCE	SOURCE	IDENTIFIER
Phusion High-Fidelity PCR kit (for cloning of Fz5 double mutants)	Thermo Fischer Scientific	Cat# F553L
T4 DNA Ligase Reaction Buffer (for cloning of gRNA zDHHC5)	New England BioLabs	Cat# B0202S
T4 DNA Ligase (for cloning of gRNA zDHHC5)	New England BioLabs	Cat# M2020S
CutSmart Buffer (for cloning of gRNA zDHHC5)	New England BioLabs	Cat# B7204
BbsI-HF (for cloning of gRNA zDHHC5)	New England BioLabs	Cat# R3539S
Lipofectamine 3000 Transfection Reagent	Invitrogen	Cat# L3000015
AMAXA nucleofection	Lonza Bioscience	Cat# VCA-1003 (cell lines), VPG-1003 (culture rat neurons)
EZ-Link HPDP-Biotin	Thermo Fischer Scientific	Cat# 21341
Streptavidin Agarose	Pierce	Cat# 10178163
Amplify Fluorographic Reagent	Amersham	Cat# NAMP100
Hyperfilm MP	Amersham	Cat# 28906844
EZ-Link Sulfo-NHS-Biotin	Thermo Fischer Scientific	Cat# 21338
GFP-Trap Agarose	Chromotek	Cat# gta-20
Protein A/G Magnetic Beads	Pierce	Cat# 88802
Protein A/G PLUS-Agarose	Santa Cruz Biotechnology	Cat#sc-2003
FluorSave reagent	Calbiochem	Cat# 345789-20
Fluoromount-G Mounting Medium	Thermo Fischer Scientific	Cat# 00-4958-02
BCA Protein Assay kit	Thermo Fischer Scientific	Cat# 23225
DC Protein Assay kit	Bio-rad	Cat# 5000116
ECL western blotting Detection Reagent	Amersham	Cat# RPN2106
Click-iT Protein Reaction Buffer Kit	Thermo Fischer Scientific	Cat# C10276
Experimental models: Cell lines		
Human: HEK293 embryonic kidney cells	ATCC	Cat# CRL-1573 RRID: CVCL_0045
Rat: NRK epithelial cells	ATCC	Cat# CRL-6509 RRID: CVCL_3758
Mouse: neuroblastoma NB2a cells	ATCC	Cat# CCL-131 RRID: CVCL_0470
Experimental models: Organisms/strains		
Rat: E18 Sprague-Dawley (embryos for hippocampal neurons)	Charles River	RRID: MGI:5651135
Mouse: C57BL/6	The Jackson Laboratory	RRID: MGI:2159769
Oligonucleotides		
Primer: 3CS -Fz5 Fw 5′-CACCAGCCGCAGCAGCAGCCGCCCGCG-3’ Rv 5′-CGCGGGCGGCTGCTGCTGCGGCTGGTG-3′	This paper	N/A
Primer: C537-538S Fw 5’-GTTTCACCAGCCGCAGCAGCTGCCG-3’ Rv 5’-CGGCTGGTGAAACGCCGCCACGACT-3’	This paper	N/A
Primer: C537-539S Fw 5’-TGGCGGCGTTTCACCAGCCGCAGCTG-3’ Rv 5’-GTGAAACGCCGCCACGACTCCACCGT-3’	This paper	N/A
Primer: C538-539S Fw 5’-CACCAGCCGCTGCAGCAGCCGCCCGC-3’ Rv 5’-TGCAGCGGCTGGTGAAACGCCGCCACGA-3’	This paper	N/A
Primer: gRNA zDHHC5 Fw 5’-CACCGATTCCTGGGTCCATAAAGGGT-3’ Rv 3’- TAAAACCCTTTATGGACCCAGGAATC-5’	This paper	N/A

(*Continued on next page*)

Continued

REAGENT or RESOURCE	SOURCE	IDENTIFIER
Recombinant DNA		
Plasmid: Fz5-HA	Prof Xi He, Harvard Medical School	N/A
Plasmid: Dvl1-HA	Our laboratory	Krylova et al.[66]
Plasmid: Fz5-SEP	This paper	N/A
Plasmid: zDHHC5-myc	Prof Akio Kihara, Hokkaido University	N/A
Plasmid: zDHHC8-myc	Prof Akio Kihara, Hokkaido University	N/A
Plasmid: Cas9	Dr Emmanouil Metzakopian, University of Cambridge	N/A
Plasmid: TCFΔN	Prof Hans Clevers, Hubrecht Institute	N/A
Plasmid: gRNA DHHC5	This paper	N/A
Plasmid: pRK5-mFzd1-1D4	Addgene	RRID: Addgene_42263
Plasmid: pRK5-mFzd2-1D4	Addgene	RRID: Addgene_42264
Plasmid: pRK5-mFzd3-1D4	Addgene	RRID: Addgene_42265
Plasmid: pRK5-mFzd4-1D4	Addgene	RRID: Addgene_42266
Plasmid: pRK5-mFzd5-1D4	Addgene	RRID: Addgene_42267
Plasmid: pRK5-mFzd6-1D4	Addgene	RRID: Addgene_42268
Plasmid: pRK5-mFzd7-1D4	Addgene	RRID: Addgene_42269
Plasmid: pRK5-mFzd8-1D4	Addgene	RRID: Addgene_42270
Plasmid: pRK5-mFzd9-1D4	Addgene	RRID: Addgene_42271
Plasmid: pRK5-mFzd10-1D4	Addgene	RRID: Addgene_42272
Plasmid: LRP6	Addgene	RRID: Addgene_27242
Plasmid: MesD	Prof Bernadette Holdener, Stony Brook University	N/A
Plasmid: EGFP-actin	Prof Yukiko Goda, Okinawa Institute of Science and Technology	N/A
Plasmid: RFP-actin	Dr Gary Wayman, Washington State University	N/A
Software and algorithms		
GPS Palm 2021	Ning et al.[33]	http://gpspalm.biocuckoo.cn/
UNIPROT Universal Protein Resource	The UniProt Consortium	RRID: SCR_002380
InterPro	European Bioinformatics Institute	RRID: SCR_006695
Volocity 3D Image Analysis Software Version 6.3	PerkinElmer	RRID: SCR_002668
GraphPad Prism Version 9	GraphPad	RRID: SCR_002798
SPSS Statistics	IBM	RRID: SCR_019096
Image Lab Software	Bio-Rad	RRID: SCR_014210
ImageJ	U.S. National Institutes of Health	RRID: SCR_003070
Biorender	Biorender	RRID: SCR_018361

RESOURCE AVAILABILITY

Lead contact

Further information and requests for resources and reagents should be directed to the lead contact, Prof Patricia C. Salinas (p.salinas@ucl.ac.uk).

Materials availability

Plasmids generated in this study are available upon request to the lead contact.

Data and code availability

- Data reported in this paper will be shared by the lead contact upon request.
- This paper does not report original code.
- Any additional information required to reanalyze the data reported in this paper is available from the lead contact upon request.

EXPERIMENTAL MODEL AND STUDY PARTICIPANT DETAILS

Cell cultures

HEK293, NRK and NB2a cells were grown in DMEM supplemented with 10% v/v fetal bovine serum (FBS) and 1% v/v penicillin/streptomycin. Cells were cultured at a density of 180 cells/mm^2 on glass coverslips for immunofluorescence analyses or at 230-280 cells/mm^2 on 60mm Petri dishes for biochemistry and maintained at 37°C and 5% CO_2.

Animal use

Sprague-Dawley rat embryos were used to isolate primary hippocampal neurons. In addition, hippocampal or intestinal lysates of C57BL/6 wild-type mice were obtained for ABE assays or to isolate synaptosomes. Analyses of synapses were also performed with brain sections from mice. All experiments on animals were performed as stated under personal and project licenses granted by the UK Home Office, in compliance with the Animals (Scientific Procedures) Act 1986 and following institutional ethical review.

Animals were housed in individually ventilated cages with sufficient bedding, together with littermates of the same sex. Whenever possible, animals were not singly housed. Animals had ad libitum access to water and food and were checked at least daily for health monitoring. Animals were exposed to a 12-hour light/12-hour dark cycle, with light intensity between 350-400 lux. The temperature of the room was maintained between 20-24°C with relative humidity at 55 ± 10%. Ambient noise did not exceed 50dBA. A microbiological surveillance program was in place to ensure the health of animals.

Primary hippocampal neuronal cultures

Primary hippocampal cultures were prepared from embryonic day 18 (E18) Sprague-Dawley rat embryos as described previously.[67] Cells were cultured at a density of 50-150 cells/mm^2 for immunofluorescence analyses or at 250 cells/mm^2 for biochemical assays and maintained at 37°C and 5% CO_2 in neurobasal media supplemented with N-2 (1X), B-27 (1X), L-glutamine (1mM) and glucose (10mM). Neurons were used at 12-14 days *in vitro* (DIV).

Intracerebroventricular (ICV) injections

Both male and female wild-type mice were used for ICV injections. These animals were not previously used for procedures and were healthy. Littermates were randomly assigned to experimental groups. Ultra-purified high-titer viruses (>10^{12} viral particles/ml) were used for injections. The lateral ventricles of P0-P1 pups were injected with adeno-associated virus serotype 9 (AAV9) to express *EGFP* only, or *EGFP* and *WT-Fz5* or *3CS-Fz5* (separated by a 2A self-cleaving peptide; P2A), as previously described[68] with minimal variations. Injection sites were located halfway between the Lambda and Bregma sutures approximately 1mm lateral of the sagittal midline. Up to 2.5 μl of the virus was injected into each ventricle to a depth of 2.5μm from the surface of the mouse's head.

Enriched environment (EE) conditions

EE experiments were carried out as previously described[61] with one-month-old mice exposed to EE for three weeks. In brief, experimental mice were caged in groups of three in bigger cages equipped with three running wheels per cage, toys, climbing walls, hiding spaces and extensive nesting material. Positions of toys were re-arranged every week. In contrast, control littermate males were singly housed in standard mouse cages with basic nesting material.

METHOD DETAILS

Bioinformatics analyses

The GPS Palm 2021 software was used to obtain predicted S-acylation sites on Frizzled receptors. These sites were determined by the software automatically using the protein sequences of Frizzled receptors found on UniProt. InterPro was then used to characterize the domains on which cysteines predicted to be S-acylated were found.

Cell line transfection

HEK293 and NB2a cells were transfected using Lipofectamine 3000 according to the manufacturer's protocol. Briefly, in each well of a 6-well plate, 2.5 μg DNA was diluted in 125 μl Opti-MEM medium and 5 μl p3000 reagent was added. The DNA master mix was combined with 1 μl lipofectamine 3000 reagent diluted in 125 μl Opti-MEM medium and incubated for 15 mins at room temperature. 250 μl of DNA/lipofectamine mix was then added to cells. 24 hours later, the medium containing the transfection mix was switched to

fresh Opti-MEM medium. For NB2a neuronal differentiation, cells were treated five hours after transfection with 1mM dibutyryl-cyclic-AMP for 48 hours.[66]

NRK cells were transfected by AMAXA nucleofection following the manufacturer's instructions. Briefly, cells were pelleted after trypsinization and $1x10^6$ cells per condition were resuspended in 100 μl of WT-EM transfection solution. Cells were gently mixed with up to 5 μg of plasmid DNA and immediately transferred to manufacturer-supplied cuvettes for nucleofection using the X-01 program of the Lonza nucleofector device. After nucleofection, 500 μl of pre-equilibrated DMEM medium was added to each cuvette and cells were collected using a thin Pasteur pipette for plating.

Transfection of primary neuronal cultures

Hippocampal neurons were transfected using calcium phosphate at 5-7 DIV or by AMAXA nucleofection before plating. For calcium phosphate transfection, 5 μl of 2.5M $CaCl_2$ combined with up to 2.5 μg of DNA and volumed to 50 μl with sterile water was mixed with 50 μl 2X HEPES buffered saline (HeBS). The DNA/$CaCl_2$/HeBS mix was left in the dark for 20 mins for complexes to form. 100 μl of the mix was then added to each well of a 6-well plate for 10 mins. For AMAXA nucleofection, the manufacturer's instructions were followed and the protocol was similar to the nucleofection of NRK cells, except the G-13 program was used on the nucleofector device.

High-frequency stimulation (HFS)

For HFS studies, 13 DIV cultured neurons were electrically stimulated using a Grass48 stimulator (Grass Instruments) via two Ag/AgCl electrodes. A regular stimulation pattern comprising trains of 400 ms containing 20 consecutive pulses (10 ms each) at 50 Hz was delivered for 1 hour at 37°C, with a 5 sec interval between trains.

Chemical long-term potentiation (cLTP)

Glycine was used to induce cLTP in cultured hippocampal neurons as previously described with minimal modifications.[21] Neurons were incubated in a control solution (125mM NaCl, 2.5mM KCl, 1mM $MgCl_2$, 2mM $CaCl_2$, 33mM D-glucose, 5mM HEPES, 20μM D-APV, 3μM strychnine, 20μM bicuculline and 0.5μM TTX; pH 7.4) for 20 mins before stimulation. To induce cLTP, the same solution was then used for 10 mins but with glycine (200μM) and without $MgCl_2$, TTX and D-APV. Neurons were subsequently returned to control solution for 50 mins to allow potentiation to occur before they were lysed to perform the ABE assay. All steps before cell lysis were performed at 37°C.

Chemical long-term depression (cLTD)

Hippocampal neurons were subjected to NMDA-mediated cLTD.[69] Neurons were first incubated in a control solution (125mM NaCl, 2.5mM KCl, 2mM $MgCl_2$, 2mM $CaCl_2$, 33mM D-glucose, 5mM HEPES, 1μM strychnine and 0.5μM TTX; pH 7.4). For cLTD induction, fresh solution was applied with 50μM NMDA and without $MgCl_2$ for 10 mins. Neurons were then returned to fresh control solution for 30 mins, before cell lysis to perform the ABE assay. All steps before cell lysis were performed at 37°C.

Synaptosome preparation

Synaptosomes were prepared as previously described[70] with minor modifications. Adult mouse brains were homogenized in sucrose buffer (see Table S2) and centrifuged at 800 g for 10 mins to remove cell debris and nuclei. The supernatant was ultracentrifuged at 9,000 g for 15 mins to obtain the pellet containing crude synaptosomes, which was resuspended in sucrose buffer and layered on top of a discontinuous sucrose gradient containing 0.85/1.2M sucrose in 4mM Hepes, pH 7.4. The sucrose layers were ultracentrifuged at 82,500 g for 2 hours and synaptosomes were collected from the 0.85/1.2M interface. Synaptosomes were pelleted by ultracentrifugation at 82,500 g for 30 mins and resuspended in sucrose buffer, then treated with Triton-X for 30 mins on a rotating wheel, followed by ultracentrifugation at 82,500 g for 45 mins. The supernatant corresponded to the synaptosomal membrane fraction (SMF) whilst the pellet corresponded to the postsynaptic density (PSD), which was resuspended in sucrose buffer. All steps were performed at 4°C.

Brain section preparation

Brains from ICV-injected mice were collected 14-15 days post-injection by fixing in 4% w/v PFA for 24 hours, then immersing in 30% w/v sucrose for 2 nights. Brains were frozen in isopentane and 30 to 50 μm sagittal sections were cut with a cryostat, and then stored at -20°C.

Pharmacological treatments

To inhibit S-acylation pharmacologically, hippocampal neurons or HEK293 were treated with 100 μM 2-BP or DMSO vehicle control for 1 hour, or with 20 μM CMA or DMSO vehicle control for 6 hours. To block protein translation to examine the rate of Fz5 degradation, NRK cells were treated with 50 μg/ml cycloheximide or DMSO vehicle control for different time points (0, 30, 60 or 120 mins). For Wnt7a treatments, hippocampal neurons or HEK293 were treated with recombinant Wnt7a (200 ng/ml) or with DMSO vehicle control for 3 hours.

Acyl-biotin exchange (ABE) assay

ABE assays were performed using lysate from HEK293, hippocampal neurons, mouse hippocampi or mouse intestines as previously described.[71] In brief, hippocampi or cells were homogenized using a tissue homogenizer (for hippocampi) or by passing through 25G

Please cite this article in press as: Teo et al., S-acylation of the Wnt receptor Frizzled-5 by zDHHC5 controls its cellular localization and synaptogenic activity in the rodent hippocampus, Developmental Cell (2023), https://doi.org/10.1016/j.devcel.2023.07.012

needles (for cells) with ABE lysis buffer (Table S2) supplemented with 10mM N-ethylmaleimide (NEM), protease inhibitors (25μg/ml pepstatin A, 25μg/ml leupeptin, 25μg/ml antipain, 25μg/ml chymostatin, 2mM PMSF) and 1.7% Triton X-100. Subsequent steps included an overnight blockade of free thiols with 10mM NEM, cleavage of the cysteine-fatty acid thioester linkages with hydroxylamine (NH_2OH) and labeling of newly exposed thiols with HPDP-biotin. After each step, chloroform-methanol precipitations were performed to yield protein free of other agents. Finally, biotin-conjugated S-acylated proteins were affinity-purified using streptavidin–agarose beads then eluted from the beads using 2.5x SDS Laemmli buffer supplemented with 250mM DTT and used for western blot analyses.

Metabolic labeling with [^{3}H]-palmitate

HEK293 transfected with Fz5-HA were metabolically labeled with [^{3}H] palmitate (1mCi/ml) for 4 hours one day after transfection. Cells were lysed in lysis buffer (50mM Tris, 150mM NaCl, 5mM EDTA, 1% Triton X-100, pH 7.4) supplemented with protease inhibitors (10μg/ml pepstatin A, 10μg/ml leupeptin, 10μg/ml N^{α}-tosyl-lysine chloromethyl ketone, 10μg/ml chymostatin, 2mM PMSF), then immunoprecipitated (IP) with anti-HA antibody using protein A/G agarose beads. IP samples were separated by 10% SDS-PAGE and 10% of the samples were used for western blot analyses to measure the level of immunoprecipitated Fz5-HA. The remaining samples were used for X-ray film exposure at −70 °C for 28-32 days. For fluorography, gels were treated with Amplify Fluorographic Reagent for 30 min, dried under vacuum, and exposed to Hyperfilm MP. Duplicate gels were treated with 1M hydroxylamine (NH_2OH; pH 7.0) for 18 hours at room temperature, followed by exposure to film as above.

Click Chemistry assay

Click Chemistry was performed as previously described.[72] Serum-free DMEM (for HEK293) or neurobasal maintenance media (for hippocampal neurons) was first supplemented with 5% w/v fatty acid-free BSA, followed by the addition of palmitic acid-alkyne (or vehicle control) to a final concentration of 100 μM. The medium containing BSA/palmitic acid-alkyne mix was sonicated continuously for 15 minutes, then left at room temperature for 15 minutes to form complexes. Cells were washed once with PBS and incubated overnight for 20 hours with the complex mix to allow metabolic incorporation of palmitic acid-alkyne. The next day, cells were lysed in ABE lysis buffer without EDTA (see Table S2). Proteins modified with palmitic acid-alkyne were selectively conjugated to biotin-azide (Click reaction) using the Click-IT kit following the manufacturer's instructions. Biotin-labeled proteins were then affinity purified using streptavidin agarose beads, eluted using 2.5x SDS Laemmli buffer supplemented with 250mM DTT and used for western blot analyses.

Surface biotinylation

Surface biotinylation experiments were performed as previously described.[20] Cells in 60mm Petri dishes were first placed on an ice block for 10-20 mins to stop membrane trafficking, then washed with ice-cold PBS containing 1mM $CaCl_2$ and 0.5mM $MgCl_2$ and treated for 30 mins with 0.25mg/ml EZ-Link Sulfo-NHS-LC-LC-Biotin (membrane impermeable biotin) to biotinylate surface proteins. Washes with 10mM glycine in PBS were performed to neutralize excess biotin. Each dish was subsequently lysed with 500μl RIPA buffer (see Table S2). Streptavidin-agarose beads were used to immunoprecipitate biotinylated proteins. Beads were treated with 2.5x SDS Laemmli buffer supplemented with 250mM DTT to elute bound proteins for western blot analyses.

Fz5;Fz5 and Fz5;Dvl1 co-immunoprecipitation

Fz5;Fz5 and Fz5;Dvl1 co-immunoprecipitation (co-IP) experiments were performed in HEK293 transfected with WT-Fz5 or 3CS-Fz5 with a super-ecliptic pHluorin (SEP) tag on its N-terminus, plus Fz5-HA or Dvl1-HA respectively. GFP-trap beads, which recognize numerous GFP variants including SEP, were then used according to the manufacturer's instructions. Relative levels of the co-immunoprecipitated proteins (Fz5-HA or Dvl1-HA) were calculated as a ratio of the level of Fz5-SEP immunoprecipitated.

Fz5;LRP6 co-immunoprecipitation

Fz5;LRP6 co-immunoprecipitation experiments were performed in HEK293 transfected with WT-Fz5-HA plus LRP6 and its chaperone protein MesD, or with 3CS-Fz5-HA plus LRP6 and MesD. 36 hours after transfection, Wnt7a treatment was performed before cells were lysed. 1 mg of protein was then added to 4.5 μg of rabbit anti-HA antibody (or IgG isotype control) overnight at 4°C on a rotating wheel to form complexes. The next day, the protein-antibody complex was added to protein A/G magnetic beads for 2 hours at room temperature with rotation to immunoprecipitate Fz5-HA complexes, which were eluted using 2.5X SDS Laemmli buffer supplemented with 250mM DTT. western blot analyses were performed with rat anti-HA and rabbit anti-LRP6 antibodies. Relative levels of co-immunoprecipitated LRP6 (IP minus IgG) were calculated as a ratio of the level of Fz5-HA immunoprecipitated.

Antibody feeding

NRK cells expressing *WT-Fz5-HA* or *3CS-Fz5-HA* were placed on an ice block for 15 mins to stop membrane trafficking. Anti-HA antibodies were diluted at 1:500 in ice-cold DMEM maintenance media and added to the cells (still on ice) for 30 mins to allow antibody binding to the extracellular HA tag of Fz5 receptors (corresponding to surface Fz5). Cells were then washed 3 times with ice-cold PBS and immediately fixed with ice-cold PFA as a control (t=0) or placed in pre-equilibrated warm DMEM and returned to a 37°C incubator for 15 mins, 30 mins or 60 mins to allow for receptor endocytosis for different durations. These cells were subsequently fixed with warm 4% w/v PFA.

Please cite this article in press as: Teo et al., S-acylation of the Wnt receptor Frizzled-5 by zDHHC5 controls its cellular localization and synaptogenic activity in the rodent hippocampus, Developmental Cell (2023), https://doi.org/10.1016/j.devcel.2023.07.012

Fluorescent recovery after photobleaching (FRAP)

For FRAP experiments, NRK cells expressing *WT-Fz5-SEP* or *3CS-Fz5-SEP* were cultured with DMEM without phenol red after transfection to reduce background fluorescence. Cells were imaged at 60x magnification using a Leica TCS SP8 inverted confocal microscope with its external chamber equilibrated at 37°C. Super-ecliptic pHluorin (SEP) is a GFP variant that does not fluoresce at the acidic pH of intracellular vesicles but emits fluorescence at neutral pH extracellularly.[51] Therefore, the fluorescence signal detected was from Fz5 receptors at the cell surface. A baseline of 15 single stack images (82x82μm) was taken every 0.25 sec before bleaching. To bleach the fluorescence signal, samples were flashed 10 times with 100% laser power every 0.25 sec in three small areas of the field of view: outside the cell (blank), at the edge of the cell (for quantification of fluorescence recovery), in the middle of the cell. Fluorescence recovery was measured by imaging at the following intervals: 1 image/0.269 sec for the first 13.18 sec; 1 image/sec for the next 30 sec; 1 image/5 sec for the next 60 sec (total=103.18 sec). The total recovery in fluorescence intensity corresponds to the mobile fraction, whilst the immobile fraction is calculated by (1 – mobile fraction).

Staining for immunofluorescence analyses

Staining was performed using standard immunofluorescence procedures. Briefly, cell lines were rinsed with warm PBS and fixed in 4% w/v PFA for 20 mins at room temperature. When fixing hippocampal neurons, 4% w/v PFA was supplemented with 4% w/v sucrose. After fixation, cultured cells were permeabilized with 0.05% v/v Triton X-100 in PBS for 5 mins (hippocampal cultures) or with 0.1% v/v Triton X-100 in PBS for 10 min (cell lines). Cultured cells were then placed for at least 1 hour in blocking buffer (5% w/v BSA/PBS for hippocampal neurons, 2% w/v BSA/PBS for cell lines). Primary antibodies were diluted in 1% w/v BSA/PBS (hippocampal neurons) or 0.05% w/v BSA/0.01% v/v Triton X-100/PBS (cell lines) and added overnight at 4°C. The following day, secondary antibodies were diluted in 1% w/v BSA/PBS and added for 1 hour in the dark. FluorSave mounting medium was used for mounting on glass microscope slides. Samples were placed at 4°C or at -20°C for short- or long-term storage respectively.

For brain slices, permeabilization and blocking were performed for 3 hours at room temperature in blocking buffer (10% w/v donkey serum/0.5% v/v Triton X-100 in PBS). Primary antibodies were then diluted in blocking buffer and added to slices overnight at 4°C. The next day, secondary antibodies were diluted in blocking buffer and added for 3 hours in the dark. Brain slices were mounted on glass microscope slides with Fluoromount-G medium and stored at -20°C.

Live staining

To evaluate surface levels of WT-Fz5-HA or 3CS-Fz5-HA receptors in hippocampal neurons expressing these constructs, live staining was performed. Cells were incubated with rat anti-HA antibody for 10 mins at 37°C, followed by PFA fixation for 20 mins and incubation with a secondary antibody against rat for 1 hour. Standard immunofluorescence procedures were then followed, including blocking, permeabilization, and staining for other proteins such as GFP.

Confocal imaging

Cultured cells were imaged with an Olympus FV1000 inverted confocal microscope or a Leica TCS SP8 confocal microscope. Brain slices were imaged with a Leica TCS SP8 confocal microscope only. On both microscopes, an oil-immersion 60x (NA 1.35) objective was used to acquire images at 207 nm/pixel, with 6-12 z-steps of 0.2μm imaged. For experiments using cultured cells, 7-15 images from at least 3 independent biological replicates were acquired. For brain slices, a minimum of 6 images from 3 slices were acquired for each animal.

Protein extraction and western blot analyses

Protein lysates were obtained from cell lines, primary neurons or mouse hippocampi using the appropriate lysis buffer (Table S2) supplemented with protease and phosphatase inhibitors. Mouse hippocampi were also homogenized and sonicated twice (30 sec each) to break tissue and shear DNA. Samples were then centrifuged at 14,000 g for 10 mins at 4°C. The supernatant was collected for protein quantification using the BCA kit according to the manufacturer's instructions. The BCA assay was incompatible with samples lysed in sucrose buffer (Table S2), for which the DC protein assay was used.

After adjusting protein concentrations, loading buffer was added and the samples were incubated at 65°C for 10 mins to denature proteins. Protein extracts were resolved on 8% or 10% SDS-page gels. Nitrocellulose membranes were blocked for at least 1h at room temperature in 5% w/v milk or 5% w/v BSA, then incubated with primary antibodies overnight at 4°C. The next day, membranes were incubated with HRP-conjugated secondary antibodies for 60 mins at room temperature. To visualize chemiluminescence signals ECL substrate was added to membranes and a Chemidoc with ImageLab software was used before quantification by densitometric analysis using ImageJ.

QUANTIFICATION AND STATISTICAL ANALYSIS

Image analyses

Volocity software was used to design protocols for the quantification of all confocal images as previously described.[73] When possible, analyses were carried out blind to the experimental condition/genotype. Similar criteria were used to identify puncta of proteins by thresholding according to two main features: fluorescence intensity and minimum/maximum object size. Colocalized puncta,

defined as the puncta of one protein in one confocal channel overlapping by at least 1 pixel within the bounds of another in a single plane, were identified automatically by the software.

Statistical analyses

Statistical analyses were performed with Prism software or SPSS. For all experiments, each animal or culture was considered an independent experimental unit except for FRAP live-imaging and antibody-feeding experiments, in which each cell was treated as an independent experimental unit. The number of independent experimental units analyzed is indicated in the figure legends.

Normality was assessed using Shapiro-Wilk or Kolmogorov-Smirnov tests. Normally distributed data were analyzed using two-tailed unpaired student's t-test for two conditions, one-way ANOVA for three or more conditions, or two-way ANOVA for datasets with two independent variables. For non-normally distributed data sets, one-sample t-tests or nonparametric tests such as Mann-Whitney or Kruskal-Wallis were used. If appropriate, post-hoc tests such as Tukey's and Bonferroni's were then used. All statistical tests used are detailed in the figure legends. All data in graphs were presented as mean ± SEM, except for data normalized to controls for which mean ± SD were shown, as indicated in the figure legends. Levels of significance were labeled as follows: $*p<0.05$, $**p<0.01$, $***p<0.001$.